Sensitization of knee-innervating sensory neurons by tumor necrosis factor-α activated fibroblast-like synoviocytes: an in vitro, co-culture model of inflammatory pain.

Sampurna Chakrabarti[1], Zoe Hore[2], Luke A. Pattison[1], Sylvine Lalnunhlimi[3], Charity N. Bhebhe[1], Gerard Callejo[1], David C. Bulmer[1], Leonie S. Taams[3], Franziska Denk[2*], Ewan St. John Smith[1*].

[1]Department of Pharmacology, University of Cambridge.

[2] Wolfson Centre for Age-Related Diseases, Institute of Psychiatry, Psychology & Neuroscience, and [3]Centre for Inflammation Biology and Cancer Immunology, Department of Inflammation Biology, School of Immunology & Microbial Sciences, King's College London

Total number of pages: 49

Figures: 4, Supplementary: 3

Tables: 1, Supplementary: 3

*Corresponding authors: Ewan St. John Smith, Department of Pharmacology, University of Cambridge, Tennis Court Road, Cambridge CB2 1PD, United Kingdom, Tel. +44 1223 334 048, Email: es336@cam.ac.uk

Abstract

Pain is a principal contributor to the global burden of arthritis with peripheral sensitization being a major cause of arthritis-related pain. Within the knee joint, distal endings of dorsal root ganglion neurons (knee neurons) interact with fibroblast-like synoviocytes (FLS) and the inflammatory mediators they secrete, which are thought to promote peripheral sensitization. Correspondingly, RNA-sequencing has demonstrated detectable levels of pro-inflammatory genes in FLS derived from arthritic patients. This study confirms that stimulation with tumor necrosis factor (TNF-α), results in expression of pro-inflammatory genes in mouse and human FLS (derived from OA and RA patients), as well as increased secretion of cytokines from mouse TNF-α stimulated FLS (TNF-FLS). Electrophysiological recordings from retrograde labelled knee neurons co-cultured with TNF-FLS, or supernatant derived from TNF-FLS, revealed a depolarized resting membrane potential, increased spontaneous action potential firing and enhanced TRPV1 function, all consistent with a role for FLS in mediating the sensitization of pain-sensing nerves in arthritis. Therefore, data from this study demonstrate the ability of FLS activated by TNF-α to promote neuronal sensitization, results that highlight the importance of both non-neuronal and neuronal cells to the development of pain in arthritis.

Keywords: synoviocytes, sensory neurons, pain, inflammation, tumor necrosis factor, complete Freund's adjuvant, knee

Introduction

Joint inflammation and pain are the major clinical symptoms of arthritis. Inflammation is part of the body's immune response to tissue damage and involves multiple cell types, including leukocytes and synoviocytes in synovial joints. These non-neuronal cells are either in direct contact with, or in close proximity to, the distal endings of joint-innervating dorsal root ganglion (DRG) sensory neurons, and this interaction is thought to cause peripheral sensitization and development of inflammatory pain.

During inflammatory diseases such as rheumatoid arthritis (RA), the affected joints undergo hyperplasia due to leukocyte infiltration and fibroblast-like synoviocyte (FLS) proliferation. FLS are key effectors in RA as they become active upon stimulation by inflammatory cytokines (released by macrophage-like synoviocytes, and T-lymphocytes) and secrete matrix metalloproteases (MMP) that cause joint destruction [9]. Correspondingly, single-cell transcriptional analysis of human RA-FLS, has identified distinct "destructive" and "inflammatory" FLS subgroups [17]. In addition, FLS can also support and maintain the ongoing inflammation in arthritic joints by secreting pro-inflammatory mediators themselves [9]. To better understand the inflammatory phenotype of FLS, several studies have used cytokine stimulation (e.g. interleukin 1β, IL-1β, or tumor necrosis factor-α, TNF-α) to robustly induce inflammation [14,27,30,40]. "Inflamed" FLS have been utilized in co-culture systems to dissect the complex interaction between FLS and other cell types in the joint environment. Co-culture of human RA-FLS with T-lymphocytes [7,11,37,67] or macrophages/monocytes [6,8,15] has been found to increase the concentration of prostaglandin (PG) E_2, IL-6, IL-8, MMP-1 and MMP-3 in the culture medium. Furthermore, upregulation of these pro-inflammatory mediators in culture supernatants was inhibited by anti-TNF-α [11,55] and anti-IL-6 antibodies [55].

However, most co-culture studies have focused on immune interactions during joint inflammation and therefore, the communication between neurons and synoviocytes is much less understood. FLS have been hypothesized to enhance nociceptive responses [64] and alter the bio-mechanical microenvironment of DRG neurons [31]. FLS derived from chronic antigen-induced arthritic (AIA) rats were observed to increase the expression of receptors associated with nociception, namely neurokinin 1, bradykinin 2 and transient receptor potential vanilloid 1 (TRPV1) in DRG neurons when co-cultured [4]. However, this study did not functionally assess modulation of DRG neuron excitability, which is a key mechanism of peripheral sensitization and hence pain. We recently showed that human osteoarthritic (OA) synovial fluid (a lubricating fluid largely secreted by FLS [5]) can cause hyperexcitability of murine sensory neurons and increase TRPV1 function [12].

To establish a suitable pro-inflammatory phenotype for our cultures, we utilized primary FLS derived from mice undergoing acute, unilateral complete Freund's adjuvant (CFA)-induced knee inflammation, which can produce neuronal hyperexcitability [13]. We also tested primary mouse knee-derived FLS treated with TNF-α, one of the main cytokines upregulated in CFA-injected mouse tissues [65] and in inflammatory arthritis [53], and validated our results in FLS derived from human OA and RA patients. The pro-inflammatory phenotype of FLS was established to test the hypothesis that after induction of inflammation, mouse knee-derived FLS will increase excitability and TRP function of knee-innervating DRG neurons (knee neurons) in an FLS-DRG neuron co-culture system.

Methods

Animals

All mice used in this study were 6-12 week old C57BL/6J mice (Envigo) randomly allocated to each experiment. Unless otherwise stated, female mice were used since in humans, females are at a higher risk for arthritic pain [28,51,62]. Mice were housed in groups of up to 5 in a temperature controlled (21 °C) room with appropriate bedding materials, a red shelter and enrichment. They were on a 12-hour/light dark cycle with food and water available *ad libitum*. Experiments in this study were regulated under the Animals (Scientific Procedure) Act 1986, Amendment Regulations 2012. All protocols were approved by a UK Home Office project license granted to Dr Ewan St. John Smith (P7EBFC1B1) and reviewed by the University of Cambridge Animal Welfare and Ethical Review Body.

Knee injections

Under anesthesia (100 mg/kg ketamine and 10 mg/kg xylazine, intra-peritoneally) mice were injected intra-articularly through the patellar tendon into each knee with the retrograde tracer, fast blue (FB, 1.5 µl 2% in 0.9% saline, Polysciences) or into the left knee with 7.5 µl CFA (10 mg/ml, Chondrex). Vernier's calipers were used to measure knee width (as before [13]) pre- and 24-hour post-CFA injection.

109 Isolation and culture of FLS

110

111 24-hours after CFA injection into the knee, mice were killed by cervical dislocation and
112 decapitation. Knee joints were exposed by removing the skin, then the quadriceps muscles were
113 resected in the middle and pulled distally to expose the patellae. Patellae were then collected by
114 cutting through the surrounding ligaments, as described before [25], in phosphate-buffered saline
115 (PBS) and then transferred into one well of a 24-well plate with FLS culture media containing:
116 Dulbecco's Modified Eagle Medium F-12 Nutrient Mixture (Ham) (Life Technologies), 25% fetal
117 bovine serum (Sigma), 2 mM glutamine (Sigma) and 100 mg/ml penicillin/streptomycin (Life
118 Technologies). Cells took approximately 10 days to grow to 70% confluency; medium was
119 changed every other day. For P1, FLS were trypsinized with 1% trypsin (Sigma), re-suspended in
120 FLS culture media and transferred into two wells of a 6-well plate. FLS from two animals were
121 combined at P2. For subsequent passages, FLS were transferred into 60 mm dishes. Contralateral
122 (Contra) and CFA-injected knees/cells (Ipsi) were kept separate at all stages. The cells were
123 maintained in a humidified, 37 °C, 5% CO_2 incubator. FLS were also cultured until P5 from mice
124 that had not undergone any knee CFA injection (control). A random selection of these dishes, from
125 three separate biological replicates, was incubated for 24 to 48-hours (as per experimental design)
126 in culture medium with recombinant mouse TNF-α (10 ng/ml from a stock solution of 100 μg/ml
127 made up in 0.2 % bovine serum albumin and sterile PBS, R&D systems, aa-80325) to stimulate
128 release of inflammatory mediators (TNF-FLS) [29].

129

130 Culture of Raw 264.7 cells

131

132 Raw 264.7 cells (EACC) were cultured in medium containing Dulbecco's Modified Eagle Medium
133 F-12 Nutrient Mixture (Ham) (Life Technologies), 10% fetal bovine serum (Sigma), 2 mM
134 glutamine (Sigma) and 100 mg/ml penicillin/streptomycin (Life Technologies). Cells were
135 maintained in a humidified 37 °C, 5% CO_2 incubator. This macrophage-like cell line [59] was used
136 to assess the level of macrophage contamination in FLS cultures.

137

138 RNA extraction and reverse transcriptase – quantitative/ polymerase chain reaction (RT-q/PCR)
139 of mouse FLS

140

141 For all conditions, RNA was extracted from two 60 mm dishes (Thermo Fisher) of FLS (various
142 passages) and from one T-25 flask (Greiner Bio-one) of Raw 264.7 cells at P3 using the RNeasy
143 Mini Kit (Qiagen). 500 ng of the extracted RNA was used to synthesize cDNA using a High
144 Capacity cDNA RT kit (Applied Biosystems) following the manufacturer's guidelines, using a
145 T100 Thermal Cycler (Bio-Rad). The resultant cDNA was diluted to a 1:5 ratio with nuclease free
146 water and quantitative PCR (qPCR) was performed using a StepOnePlus Real Time PCR system,
147 following the manufacturer's guidelines on settings (Applied Biosystems) using TaqMan probes
148 (Thermo Fisher) (Supplementary Table 1 listing genes of interest analyzed in this study). The
149 fluorescence intensity of samples was captured during the last minute of each cycle. All reactions
150 were run in triplicate with appropriate negative controls with water containing no cDNA.

151 For RT-qPCR reactions, data were obtained as Ct values (the cycle number at which fluorescent
152 signals emitted by the TaqMan probe crossed a threshold value). Only Ct values below 35 were

153 analyzed to determine ΔCt values by subtracting the Ct of *18S* ribosomal RNA from the Ct of
154 target gene [41]. ΔCt values of target genes were subtracted from average ΔCt values of their
155 controls to calculate ΔΔCt, followed by 2^(- ΔΔCt) to calculate fold change [39].

156 FLS gene expression was also assessed by RT-PCR. DreamTaq Polymerase (Thermo Fisher) was
157 used to amplify a section within the open reading frames of various genes from 5 ng template
158 cDNA. The sequences of designed oligonucleotides (Sigma) are listed in Supplementary Table 1.
159 Negative controls (using water/RNA as the template) were performed for each biological sample
160 with a randomly selected primer pairing. PCR products were resolved on 2% agarose containing
161 1X GelRed Nucleic Acid Stain (Biotum) and imaged with a GeneFlash Gel Documentation System
162 (Syngene). A randomly selected subset of reactions was repeated with 2.5 ng template cDNA to
163 ensure reproducibility. Densitometry analyses were performed using ImageJ Software (NIH)
164 where relative expression was determined by dividing the band intensity of each gene by that of
165 the housekeeping gene, *18S* ribosomal RNA, for each biological replicate.

166

167 Cytokine antibody array

168

169 Before RNA extraction, 2 ml of culture media from P5 Contra, Ipsi, control and TNF-FLS (48-
170 hour) were collected and stored at -80 °C until use. Culture medium was pooled from three cultures
171 for each of the four conditions and assayed (undiluted) for the presence of 40 inflammatory
172 mediators using Mouse Inflammatory Antibody Array Membranes (ab133999, Abcam) according
173 to the manufacturer's instructions. Chemiluminescence was imaged using a BioSpectrum 810

174 imaging system (UVP) with 3 min exposure. Location of the 40 cytokines detected by the array
175 membranes are shown in Supplementary Table 2.

176 Densitometry of the spots in the array membranes was performed using ImageJ software (NIH).
177 Briefly, the mean gray value of each spot was measured from all membranes using the same
178 circular region of interest. The spots of interests were then subtracted from background (average
179 of all negative control spots) and normalized to the positive control spots of the reference
180 membrane (control FLS media). A fold change value was obtained by dividing normalized
181 intensities of the membrane of interest and the control membrane, analyte-by-analyte.

182

183 Culture of human FLS

184

185 FLS was obtained from 1 OA and 3 RA female patients (age range 61 – 81 years, see
186 Supplementary Table 3 for detailed patient information) with approval from local ethics committee
187 (07/H0809/35). These were then seeded separately at 10,000/well in 200 µl of DMEM media
188 (Sigma) supplemented with 10% FCS (Fisher Scientific), 100 units/ml of Penicillin/Streptomycin
189 (Fisher Scientific), 2% glutamine (Thermo Fisher) and fungizone (Thermo Fisher) into a 96-well
190 flat bottom plate (Starlab). The plate was incubated overnight at 37 °C to allow for SF attachment
191 and the following morning media was replaced with either 200µl of fresh DMEM containing 10
192 ng/ml of TNF-α (PeproTech), or fresh DMEM alone. Supernatants were collected following 24-
193 hours of incubation at 37 °C.

194

195 RNA extraction and RT-qPCR of human FLS

196

197 RNA was extracted using a RNeasy Micro Kit (Qiagen) according to the manufacturer's protocol,
198 then reverse transcribed and amplified using a slightly modified version of the Smart-seq2 method
199 [48]. Briefly, in a RNase/DNA-free fume hood 2 µl of RNA was mixed with 1 µl of dNTP mix
200 (Thermo Scientific), 1 µl of Oligo-dT primer (Merck) and 5.7 µl of RT mix, then reverse
201 transcribed on a PTC-225 Gradient Thermal Cycler (MJ Research). 15 µl of PCR mix was added
202 to the resulting cDNA and amplified according to previously established protocol. Concentrations
203 were checked on a Qubit 3.0 (Invitrogen), with values ranging from 20.4 – 45.0 ng/µl. Samples
204 were diluted to 1 ng/µl with double distilled H_2O (ddH_2O) and 1 ng was used for standard SYBR
205 Green (Roche) RT-qPCR reactions on a LightCycler480 (Roche) to probe for the genes of interest
206 (see Supplementary Table 1 for primer sequences). All primers were tested for their efficiency and
207 specificity. The mean of housekeeping genes *B2M* and *Ywhaz* was used to calculate ΔCt values.
208 All reactions were run in duplicate with water used as a negative control.

209

210 DRG neuron isolation and culture

211

212 Lumbar DRG (L2-L5, those that primarily innervate the knee) were collected from FB labelled
213 mice 7-10 days after knee injections in ice cold dissociation media containing L-15 Medium (1X)
214 + GlutaMAX-l (Life Technologies), supplemented with 24 mM $NaHCO_3$. DRG were then
215 enzymatically digested in type 1A collagenase (Sigma) and trypsin solution (Sigma) at 37 °C,
216 followed by mechanical trituration as described before [13]. Dissociated DRG neurons were plated

217 onto poly-D-lysine and laminin coated glass bottomed dishes (MatTek, P35GC-1.5-14-C) and
218 cultured either on their own (mono-culture), on a layer of FLS (co-culture, see below) or in 48-
219 hour conditioned media from TNF-FLS for 24-hours. The DRG culture medium contained L-15
220 Medium (1X) + GlutaMAX-l, 10% (v/v) fetal bovine serum, 24 mM $NaHCO_3$, 38 mM glucose,
221 2% (v/v) penicillin/streptomycin.

222

223 DRG neuron/FLS co-culture

224

225 For co-culture studies, FLS were plated onto MatTek dishes and cultured for 24-hours with FLS
226 culture media (with or without TNF-α stimulation). The next day medium was removed from FLS
227 plates, then DRG neurons were isolated as described above and plated on top of the FLS. Co-
228 culture plates were then kept in DRG culture medium for up to 24-hours for electrophysiological
229 recording.

230

231 Cell staining

232 **FLS immunocytochemistry:** FLS were plated overnight in wells of a 24-well plate, fixed with
233 Zamboni's fixative [57] for 10 min, permeabilized with 0.05 % TritonX-100 and blocked with
234 antibody diluent (0.2% (v/v) Triton X-100, 5% (v/v) donkey serum and 1% (v/v) bovine serum
235 albumin in PBS) for 30 min. The cells were then incubated overnight at 4 °C in 1:100 (in antibody
236 diluent) anti-cadherin-11 antibody (CDH-11, rabbit polyclonal, Thermo Fisher, 71-7600). Cells
237 were washed three times with PBS-tween and incubated in the conjugated secondary antibody,
238 anti-rabbit Alexa-568 (1:1000 in PBS, Thermo Fisher, A10042) for 1-hour at room temperature

239 (21 °C). The secondary antibody was washed off three times with PBS-tween and the cells were
240 incubated in the nuclear dye DAPI (1:1000 in PBS, Sigma, D9452) for 10 min. Cells were further
241 washed with PBS-tween once and imaged in PBS using an EVOS FLoid Cell Imaging Station
242 (Thermo Fisher) at 598 nm (for CDH-11) and 350 nm (for DAPI) wavelength of light. Cells
243 without primary antibody did not show fluorescence.

244 **DRG neuron/FLS co-culture live cell stain:** To visualize DRG neuron/FLS co-culture, live cell
245 imaging was performed. FLS were plated on MatTek dishes with 1:1000 (diluted in FLS culture
246 medium) CellTracker Deep Red Dye (Thermo Fisher, C34565) and incubated for 24-hours in a
247 humidified 37 °C, 5% CO_2 incubator. Dissociated DRG neurons (see above) were incubated in
248 CellTracker Green Dye (1: 1000 diluted in DRG culture media, Thermo Fisher, C7025) for 15 min
249 at room temperature (21 °C), centrifuged (16000 g, 3 min, 5415R, Eppendorf) and re-suspended
250 in fresh medium. The FLS dishes were then washed twice with PBS and the neuronal suspension
251 was plated on top of the FLS monolayer and incubated overnight in the incubator. The co-culture
252 dishes were washed with PBS and imaged the following day using an Olympus BX51 microscope
253 and QImaging camera at 650 nm (for deep red dye) and 488 nm (for green dye) wavelength of
254 light.

255

256 Whole-cell patch-clamp electrophysiology

257 DRG neurons were bathed in extracellular solution containing (ECS, in mM): NaCl (140), KCl
258 (4), $MgCl_2$ (1), $CaCl_2$ (2), glucose (4) and HEPES (10) adjusted to pH 7.4 with NaOH. Only FB
259 labelled neurons identified by their fluorescence upon excitation with a 365 nm LED (Cairn
260 Research) were recorded. Patch pipettes of 5–10 MΩ were pulled with a P-97 Flaming/Brown

261 puller (Sutter Instruments) from borosilicate glass capillaries and the intracellular solution used
262 contained (in mM): KCl (110), NaCl (10), $MgCl_2$ (1), EGTA (1), HEPES (10), Na_2ATP (2),
263 Na_2GTP (0.5) adjusted to pH 7.3 with KOH.

264 Action potentials (AP) were recorded in current clamp mode without current injection for 20 s (to
265 investigate spontaneous AP firing) or after step-wise injection of 80 ms current pulses from 0 –
266 1050 pA in 50 pA steps using a HEKA EPC-10 amplifier (Lambrecht) and the corresponding
267 Patchmaster software. AP properties were analyzed using Fitmaster software (HEKA) or IgorPro
268 software (Wavemetrics) as described before [13] and shown in Figure 3D (inset). Neurons were
269 excluded from analysis if they did not fire an AP in response to current injection. For recording
270 whole-cell voltage-clamp currents in response to TRP agonists capsaicin (1 μM from a 1 mM stock
271 in ethanol, Sigma-Aldrich), cinnamaldehyde (100 μM from a 1 M stock in ethanol, Alfa Aesar)
272 and menthol (100 μM from a 1 M stock in ethanol, Alfa Aesar), a 5 s baseline was established
273 with ECS, followed by a 5 s randomized drug application. Peak drug response was measured in
274 Fitmaster by subtracting the average of 2 s baseline immediately preceding the drug application
275 and the maximum peak response reached during the 5 s of drug application. Peak current density
276 is represented in graphs by dividing this peak response by the capacitance of the neuron. Data from
277 at least four mice were used in all conditions (with each mouse being used for at least two
278 conditions) and at least three neurons were recorded from each mouse in each category.

279

280 Ca^{2+} imaging

281 FLS or DRG neurons were incubated with the Ca^{2+} indicator, Fluo-4 AM (10 μM diluted in ECS
282 from a 10 mM stock solution in DMSO, Invitrogen) for 30 min at room temperature (21 °C).

283 Culture dishes were then washed and imaged using an inverted Nikon Eclipse T*i* microscope. Fluo-
284 4 fluorescence was excited using a 470 nm LED (Cairn Research) and captured with a camera
285 (Zyla cSMOS, Andor) at 1 Hz with 50 ms (for neurons) 250 ms (for FLS) exposure time using
286 Micro-Manager software (v1.4; NIH). Solutions were perfused in this system through a gravity-
287 driven 12 barrel perfusion system [20]. During imaging of neurons, MIP-1γ (10 and 100 ng/ml
288 diluted in ECS from a stock concentration of 0.1 mg/ml in 0.1% bovine serum albumin/sterile
289 PBS, Sigma) was applied for 20 s after establishing a baseline with ECS for 10 s. Neurons were
290 allowed to recover for 5 minutes between drug applications. 50 mM KCl was used as a positive
291 control.

292 During imaging of FLS, a 10 s baseline was established with ECS and then pH 4-7, and TRP
293 agonists, 1 μM capsaicin, 100 μM cinnamaldehyde and 100 μM menthol were applied for 10 s
294 before a wash out period of 4 min between drug applications. TRP agonist sensitivity and acid
295 sensitivity was assessed on separate dishes. Three biological repeats were conducted on separate
296 days for each condition. 10 μM ionomycin was used as a positive control after all FLS Ca^{2+}
297 imaging experiments.

298 Analysis was conducted as described before [12]. Briefly, mean grey values were extracted by
299 manually drawing around FLS or neurons in the ImageJ software. These values were then fed into
300 a custom-made R-toolbox (https://github.com/amapruns/Calcium-Imaging-Analysis-with-R.git)
301 to compute the proportion of cells responding to each drug and their corresponding magnitude of
302 response (normalized to their peak ionomycin (FLS) or KCl (neuron) response, (ΔF/Fmax); cells
303 not crossing threshold for positive controls were excluded from the analysis).

304

305 Extraction of RNA-Seq data from RA and OA patient synovial tissue samples

306

307 Publicly available single cell RNA-Seq data of synovial tissue from 51 OA and RA patients [68]
308 was used to investigate the presence of pro-inflammatory genes. For each sample, we extracted
309 the transcripts per million (TPM) values for the same genes investigated for RT-qPCR of human
310 FLS and organised data by patient ID, cell type and patient group. The 17 samples that failed or
311 were pending quality control were excluded. The remaining 151 samples were subsequently
312 plotted by dividing into two groups – OA and RA.

313

314 Statistics

315

316 Comparisons between two groups with distributed variables were performed using two-sided
317 Student's t-tests (paired if comparing two conditions of the same sample, unpaired otherwise) with
318 suitable corrections and amongst three groups using one-way analysis of variance (ANOVA)
319 followed by Tukey's post-hoc tests. Proportions were compared for categorical data using chi-sq
320 tests. Data are shown as mean ± SEM.

321

322

323

324

325

326 **Results**

327

328 1. TNF-FLS, but not FLS derived from CFA-induced inflamed knees of mice, have a pro-
329 inflammatory phenotype and secrete cytokines that activate DRG neurons.

330 Key genes have been described that act as identifiers of cultured FLS upon isolation by enzymatic
331 digestion of mouse joints [29], as well as for establishing their inflammatory phenotype. In this
332 study, we performed RT-qPCR on adherent cells (passages P2-P5) originating from mouse patellae
333 that proliferated in culture (Figure 1A, B). From P2 to P3, the expression of the macrophage marker
334 [5,29] cluster of differentiation 68 (*Cd*68, relative to the macrophage cell line RAW 267.4) was
335 significantly reduced, whereas the expression of FLS markers *Cdh11* and *Cd248* [5,29] remained
336 consistent from P2 to P5 (Supplementary Figure 1A, B showing expression of FLS marker genes);
337 the endothelial marker *Cd31* was not detected (data not shown). These results suggest that from
338 P3, cells cultured from mouse patellae were predominantly FLS and hence subsequent studies were
339 conducted on FLS from P3-P6.

340 Concurrently, to establish the pro-inflammatory phenotype of FLS, we used RT-qPCR to
341 determine the expression of the inflammatory genes *Il-6*, *Il-1r1* and *Cox-2*, as well as the
342 constitutively expressed gene *Cox-1.* When control FLS (P5, n = 3 biological replicates) were
343 stimulated with 10 ng/ml TNF-α for 48-hours, there was an upregulation of *Il-6* (fold changes:
344 Control, 1.5 ± 0.8 vs. TNF-FLS, 135.1 ± 31.1, $p = 0.006$, unpaired t-test) and *Il-1r1* (fold changes:
345 Control, 1.1 ± 0.2 vs. TNF-FLS, 3.4 ± 1.0, $p = 0.04$, unpaired t-test) expression levels, but not that
346 of *Cox-2* (fold changes: Control, 1.0 ± 0.2 vs. TNF-FLS, 0.8 ± 0.2, $p = 0.2$, unpaired t-test) or

347 *Cox-1* (fold changes: Control, 1.0 ± 0.2 vs. TNF-FLS, 0.8 ± 0.2, $p = 0.18$, unpaired t-test) (Figure
348 1C). However, when FLS derived from the inflamed knee (Ipsi, knee width, pre-CFA, 3.1 ± 0.09
349 mm vs. post-CFA, 4.1 ± 0.08 mm, $n = 6$, $p = 0.0001$, paired t-test, Supplementary Figure 1C
350 showing knee width of mice pre and post-CFA injection) of CFA injected mice were compared to
351 those of the matched contralateral knee (Contra), we did not find any changes in expression levels
352 of the genes between Contra and Ipsi FLS across P2-P5 (Figure 1C, Supplementary Figure 1C).

353 We next tested the media ($n = 3$, each) isolated from control, Contra, Ipsi and TNF-FLS against a
354 mouse inflammation antibody array (Figure 1D) to determine the levels of different secreted pro-
355 inflammatory mediators. This demonstrated that when compared to control FLS media, TNF-FLS
356 media showed presence of regulated on activation, normal T-cell expressed and secreted
357 (RANTES) and granulocyte-macrophage colony stimulating factor (GM-CSF). Additionally,
358 TNF-FLS contained higher levels of IL-6 ($p < 0.0001$), keratinocyte chemoattractant (KC, mouse
359 homolog of IL-8, $p < 0.0001$), lipopolysaccharide induced chemokine (LIX, $p < 0.0001$), stromal
360 cell derived factor 1 (SDF-1, $p < 0.0001$), fractalkine ($p < 0.0001$), monocyte chemoattractant
361 protein 1 (MCP-1, $p < 0.0001$) and macrophage inhibitory protein 1γ (MIP-1γ, $p = 0.002$) and
362 lower levels of macrophage colony stimulating factor (MCSF, $p = 0.003$) compared to control FLS
363 media (multiple t-tests with Holm-Sidak corrections, Figure 1Dii). The TNF-α concentration in
364 TNF-FLS media 48-hours after 10 ng/ml TNF-α stimulation was similar to the control media as
365 determined by the inflammatory antibody array. Mirroring the absence of pro-inflammatory gene
366 upregulation in Ipsi vs. Contra FLS, the spot intensity values of inflammatory cytokines between
367 Ipsi and Contra FLS were similar (multiple t-tests with Holm-Sidak corrections, graph not shown),
368 suggesting similar levels of secreted cytokines. Finally, when spot intensities were normalized to
369 control FLS, TNF-FLS media showed increased levels of secreted IL-6 ($p < 0.0001$, ANOVA

370 followed by Tukey's multiple comparison test) and KC ($p = 0.001$, ANOVA followed by Tukey's
371 multiple comparison test) compared to Ipsi and Contra FLS (Figure 1Diii).

372 MIP-1γ was elevated in both Ipsi and Contra FLS when compared to control and TNF-FLS (Figure
373 1Diii), perhaps indicating its role in acute, systemic inflammatory pathways. MIP-1γ has been
374 described as having a role in hyperalgesia induced by diabetic neuropathy [49] and OA-related
375 pain [19]. We find that MIP-1γ directly activates mouse DRG neurons by producing a dose-
376 dependent Ca^{2+} influx (Supplementary Figure 1D showing intracellular Ca^{2+} mobilization in DRG
377 neurons upon MIP-1γ application), which thus might be a potential mechanism for the *in vivo*
378 effects described above. However, because MIP-1γ does not have a human homolog (NCBI gene
379 database entry #20308), and thus has limited clinical potential, we did not explore this further.

380 Taken together, our data suggest that TNF-α stimulation of FLS upregulates expression of
381 canonical inflammatory markers, whereas the knee inflammation observed 24-hours after intra-
382 articular CFA injection does not correlate with a sustained pro-inflammatory phenotype of FLS
383 isolated from patellae of CFA mice. We also identify other soluble mediators secreted by TNF-
384 FLS that might be involved in FLS-DRG neuron communication. Therefore, given the pro-
385 inflammatory phenotype of TNF-FLS (and the lack of such phenotype in the FLS expanded from
386 CFA-injected knees), we focused solely on the TNF-FLS for the rest of the study.

387

388

389

390 2. TNF-α stimulated human FLS from OA and RA patients show increased expression
391 of multiple pro-inflammatory genes that were upregulated in mouse TNF-FLS.

392 In order to understand whether the identified pro-inflammatory mediators from mouse FLS are
393 important in human arthritis, we examined gene expression in human FLS. In arthritis, activated
394 FLS contribute to pathogenesis by damaging synovial membranes and secreting inflammatory
395 cytokines which in turn recruit immune cells [32,44,45]. In line with these reports, data re-plotted
396 from a recently published single-cell RNA-seq dataset of FLS from 51 OA and RA patients [68]
397 confirms detectable levels of pro-inflammatory genes *IL-6, KC, MCP-1, IL-8, IL1-R1, SDF-1* and
398 *Fractalkine* (Figure 2A), which matches our mouse data in Figure 1.

399 Furthermore, to establish whether a similar pro-inflammatory phenotype can be observed in TNF-
400 α treated human FLS as in mouse FLS, we used RT-qPCR. When four batches of human FLS
401 derived from four separate patients were stimulated with 10 ng/ml TNF-α for 24-hours, there was
402 increased expression of *IL-6* ($p = 0.02$), *KC* ($p = 0.001$), *LIX* ($p = 0.009$), *MCP-1* ($p = 0.0004$) and
403 *IL-8* ($p = 0.005$) compared to unstimulated controls (unpaired t-test) (Figure 2B). However,
404 expression of *SDF-1* ($p = 0.8$), *IL-1R1* ($p = 0.3$) and *Fractalkine* ($p = 0.3$) was not significantly
405 different in the TNF group compared to control (unpaired t-test), although for the latter two genes,
406 FLS from some patients showed considerable increase after TNF-α stimulation (Figure 2B).

407 The data presented here demonstrate the translational potential of our data derived from mouse
408 FLS (Figure 1), as well as supporting a previous study that showed increased cytokine production
409 from TNF-α stimulated human FLS from both normal and RA donors compared to unstimulated
410 ones [32].

411

412 3. TNF-FLS derived from mice increase knee-innervating DRG neuron excitability in co-
413 culture.

414 Changes in primary sensory neuron excitability underlie peripheral sensitization which drives
415 arthritis-related pain [58]. Non-neuronal cells like FLS, which are in close proximity with distal
416 terminals of knee neurons, can play instrumental roles in modulating sensory neuron excitability
417 by direct cell contact and/or secretion of pro-inflammatory cytokines. To determine neuron/FLS
418 communication in health and inflammation we compared the DRG neuronal excitability of four
419 groups: 1) knee neuron mono-culture, 2) knee neurons co-cultured with control FLS (Figure 3A,
420 B), 3) knee neurons with FLS that have been exposed to TNF media for 24-hour followed by DRG
421 culture media for 24-hours and 4) knee neurons with conditioned media from FLS that have been
422 exposed to TNF media for 48-hours to understand the role of soluble mediators in peripheral
423 sensitization. In current-clamp mode, we observed many neurons spontaneously firing AP during
424 a 20 s recording period (mostly with an intermittent firing pattern, although neurons that fired >100
425 APs had a continuous firing pattern) in groups 3 and 4. In order to statistically compare the
426 proportions, we converted our four group data into binary categories: neuron mono-culture and
427 neuron/control FLS co-culture were assigned to the class "healthy", and neuron/TNF-FLS and
428 neuron/TNF-FLS media were assigned to the class "inflamed". 19.5% of inflamed neurons
429 (neuron/TNF-FLS, 5/21; neuron/TNF-FLS media, 3/19) fired spontaneous AP compared to 2.7%
430 (neuron mono-culture, 0/19; neuron/control FLS, 1/18) of healthy neurons ($p = 0.02$, chi-sq test).
431 The mean number of APs fired (within the 20 s recorded without current injection) by neurons in
432 the neuron/TNF-FLS and neuron/TNF-FLS media categories was 31.6 ± 18.6 and 76.0 ± 62.5
433 respectively, while the neuron in the neuron/control FLS group fired 18 times. This result suggests

434 that there is a general increase in excitability of knee neurons when exposed to an FLS-mediated
435 inflammatory environment (Figure 3C, D).

436 Upon measuring the AP properties (Figure 3D inset) we found that the resting membrane potential
437 (RMP) was more depolarized in the neuron/TNF-FLS media group compared to both neuronal
438 mono-culture ($p = 0.0004$) and neuron/control FLS co-culture ($p = 0.012$), which highlights that
439 secreted pro-inflammatory factors from TNF-FLS likely act upon knee neurons to increase their
440 excitability (ANOVA followed by Tukey's post hoc comparison, Figure 3Ei). This depolarizing
441 trend in RMP was also observed when the data were divided into small and medium-large neurons
442 (Supplementary Figure 2). The other measured properties were unchanged among the four groups
443 (ANOVA followed by Tukey's post hoc comparison, Table 1, Figure 3Eii-iv).

444

445 4. TNF-FLS derived from mice increase TRPV1 function and decrease TRPA1/TRPM8
446 function of DRG neurons in co-culture.

447 DRG neurons in co-culture with inflamed FLS derived from AIA rats reportedly have increased
448 expression of TRPV1 [4]. Here we sought to investigate whether FLS can modulate knee neuron
449 responses to TRP channel agonists using whole-cell patch-clamp recordings. Knee neurons in
450 mono-culture and when co-cultured with control FLS displayed very similar responses, i.e. a mean
451 capsaicin peak current density response of 3.5 ± 1.0 pA/pF ($n = 7/19$) and 3.2 ± 0.9 pA/pF ($n =$
452 $7/18$) respectively. By contrast, knee neurons in neuron/TNF-FLS co-culture showed a trend for
453 larger magnitude of capsaicin responses (27.7 ± 9.3 pA/pF, $n = 8/21$), and those cultured with
454 TNF-FLS media had a capsaicin response of 65.8 ± 25.7 pA/pF ($n = 7/20$) which was significantly
455 larger in magnitude than neuronal mono-culture ($p = 0.02$) and neuron/control FLS co-culture (p

456 = 0.02) (ANOVA followed by Tukey's post-hoc comparison, Figure 4Ai,ii). However, no
457 difference was observed between the percentage of capsaicin responders in healthy (40.5%) vs.
458 inflamed groups (37.5%, p = 0.8, chi-sq test, Figure 4Aiii), suggesting that although TRPV1
459 channel function is sensitized in TRPV1-expressing neurons, TNF-FLS exposure does not induce
460 TRPV1 expression in neurons lacking any basal expression.

461 With regards to menthol (mono-culture, 2.4 ± 1.2 pA/pF, n = 7/19; neuron/healthy FLS, 4.8 ± 2.1
462 pA/pF, n = 6/18; neuron/TNF-FLS, 1.4 ± 1.2 pA/pF, n = 2/21; neuron/TNF-FLS conditioned
463 media, 4.0 ± 1.9 pA/pF, n = 4/20; Figure 4Bi) and cinnamaldehyde (mono-culture, 1.9 ± 0.7 pA/pF,
464 n = 10/19; neuron/healthy FLS, 2.8 ± 1.1 pA/pF, n = 4/18; neuron/TNF-FLS, 0.6 ± 0.3 pA/pF, n =
465 3/21, neuron/TNF-FLS conditioned media, 2.3 ± 1.5 pA/pF, n = 3/20; Figure 4Ci) responses, all
466 four groups showed similar mean peak current density values (Figure 4Bii, Cii). However, in
467 response to both the TRPA1 (cinnamaldehyde) and TRPM8 (menthol) agonists, the percentage of
468 responding neurons was significantly less in the inflamed group compared to healthy (menthol:
469 healthy vs. inflamed, 37.8% vs. 15%, p = 0.02, chi-sq test; cinnamaldehyde: healthy vs. inflamed,
470 43.2% vs. 15%, p = 0.006, chi-sq test, Figure 4Biii, Ciii). Taken together our data suggest that
471 "inflamed" FLS can alter TRP channel agonist response of knee neurons in co-culture.

472 Overall, our data suggest that pro-inflammatory mediators secreted from FLS are capable of
473 increasing excitability and TRPV1 function of knee-innervating DRG neurons. It has been
474 hypothesized that secretion by FLS is mediated by an increase in intracellular [Ca^{2+}] [16,35] and
475 depolarization. Furthermore, during inflammatory arthritis, FLS are located in an environment
476 with abundant algogens that have been shown to signal through the modulation of TRP channels
477 [9] and there is also mixed evidence in animals and humans for development of tissue acidosis
478 [3,24,66]. TRP channels and acid sensors in FLS can increase intracellular [Ca^{2+}] [26,35] and

479 therefore, we tested the sensitivity of mouse knee-derived FLS to a range of acidic pH stimuli, as
480 well as the prototypic TRP channel agonists, capsaicin (TRPV1), cinnamaldehyde (TRPA1) and
481 menthol (TRPM8) using Ca^{2+} imaging. We found that both control and TNF-FLS responded to a
482 range of pH solutions (pH 4.0 – 7.0) with an increase in intracellular [Ca^{2+}], with an increased
483 percentage of TNF-FLS responding to acid than control FLS at pH 5.0-6.0 (Supplementary figure
484 3). However, capsaicin (control, 3/201, TNF-FLS, 13/252), cinnamaldehyde (control, 1/201, TNF-
485 FLS, 11/252) and menthol (control, 0/201, TNF-FLS, 1/194) evoked a Ca^{2+} response in only a
486 few cells (data not shown), leading us to conclude that very few mouse FLS have functional
487 TRPV1, TRPA1 and TRPM8 ion channels. RT-PCR for control and TNF-FLS revealed expression
488 of multiple proton-sensors and low *Trpv1* expression, further validating the Ca^{2+} imaging results
489 (Supplementary figure 3). Therefore, our data supports the hypothesis of Ca^{2+} dependent secretion
490 in FLS leading to increased knee neuron sensitization and nociception.

491

492 **Discussion**

493 FLS can respond to pro-inflammatory environments and then themselves become effectors for
494 driving disease pathology, and hence are called "passive responders and imprinted aggressors" [9].
495 In support of their activated phenotype, here we demonstrate that FLS obtained from human OA
496 and RA patients and from cell-outgrowth of mouse patella can respond to TNF-α stimulation to
497 increase secretion and expression of several pro-inflammatory mediators. We used these findings
498 to establish a co-culture system, which showed that murine FLS and knee neurons can interact,
499 specifically, factors secreted by TNF-FLS increase knee neuron excitability and the magnitude of
500 the response to capsaicin, whereas the proportions of cinnamaldehyde and menthol responding
501 neurons are diminished. To the best of our knowledge, this is the first report to demonstrate FLS-

502 mediated changes in neuronal excitability in co-culture and hence directly demonstrate how FLS
503 can regulate articular neurons and in turn arthritis-related pain.

504 FLS from mouse are generally cultured by enzymatically digesting and combining excised joints
505 of fore- and hind-limbs [26,29,50,56], which assumes similarity of FLS derived from all joints.
506 However, a genome-wide study on DNA-methylation has shown that important differences exist
507 between knee and hip FLS, including of genes involved in IL-6 signalling [1]. By using a cell-
508 outgrowth method to culture mouse FLS, as previously described in humans [34] and rats [4], we
509 have avoided the biological ambiguity introduced by joint-to-joint variability. Using these FLS,
510 we investigated the expression of inflammatory genes *Il-6*, *Il-1r1* and *Cox-2*, all of which have
511 been linked to the inflammatory phenotype of FLS. In brief: stimulating human-derived FLS with
512 IL-1β increases *Cox-2* and *Il-6* expression [34]; increased *Il-6* expression is seen in FLS derived
513 from K/BxN mice and following 24-hour stimulation of healthy mouse FLS with TNF-α [29].
514 Lastly, supernatants from cultured FLS derived from rats 3-days into AIA model show increased
515 IL-6 and PGE_2 [4]. Here we observed that neither the expression level of *Il-6*, *Il-1r1, Cox-2*, nor
516 the level of secreted cytokines was upregulated in FLS derived from CFA-injected knee (our local
517 ethics review body did not permit investigation of > 24-hours following CFA injection). This is
518 possibly because the model used here is too brief to influence FLS gene expression, which is
519 supported by a previous study where FLS derived from rats with longer (3-28 days) AIA-induced
520 knee inflammation did have higher PGE_2 and IL-6 concentrations in culture supernatants
521 compared to control [4].

522 Therefore, we created a model of inflammation *in vitro* where we exposed FLS to TNF-α, a
523 cytokine that is locally upregulated within 3-hours of intra-plantar CFA injection in mice [65]. It
524 is also present in high concentrations in the synovial fluid [36,53] and tissue of OA and RA patients

525 [47,61]; along with anti-TNF-α agents being a leading treatment of RA [60]. We show that TNF-
526 α stimulated FLS display increased expression of *Il-6* and *Il-1r1* mRNA, with a concomitant
527 increase in secretion of many pro-inflammatory cytokines, including IL-6 - a finding reported
528 previously in human FLS [32] and replicated in this study. This observation is consistent with FLS
529 being effectors of inflammatory arthritis, and hence we explored the functional repercussions of
530 this pro-inflammatory phenotype by investigating the ability of "inflamed" FLS to induce
531 functional changes in nerves supplying the knee joint to drive pain.

532

533 In order to understand the effector role of FLS in driving nociception through peripheral
534 sensitization, we set up a co-culture system combining FLS and knee neurons. Studying co-culture
535 of rat FLS and DRG neurons, von Banchet *et al* showed using immunohistochemistry that
536 bradykinin 2 receptor labelling (but not that of neurokinin 1 or TRPV1) was increased when DRG
537 neurons were cultured with healthy rat FLS [4], i.e. co-culture of DRG neurons with FLS can alter
538 expression of genes associated with nociception. Therefore, we first verified that knee neurons in
539 co-culture with control FLS do not show dysregulation of excitability or TRP agonist response.
540 Then we asked whether TNF-FLS modulate knee neuron function and found using whole-cell
541 patch clamp that 23% and 16% of knee neurons in neuron/TNF-FLS co-culture and neuron/TNF-
542 FLS media (19.5 % in the combined "inflamed" condition) respectively evoked spontaneous AP
543 compared to 6% in neuron/control FLS and 0% in neuron mono-culture (2.7% in the combined
544 "healthy" condition). This suggests that TNF-FLS increase excitability of knee neurons and thus
545 contribute to arthritic pain.

546 von Banchet *et al* [4] also showed that compared to mono-culture, FLS derived from acute and
547 chronic AIA rats induced an increase in TRPV1 protein expression in DRG neurons, which can
548 also lead to sensitization and hence arthritic pain. However, we did not observe an increase in the
549 proportion of neurons responding to capsaicin between healthy and inflamed conditions, which
550 might reflect a species difference and/or difference in knee-specific neuronal population (unlike
551 in this study, von Banchet *et al* did not discriminate between knee-innervating neurons and non-
552 knee innervating neurons); however, we did observe that capsaicin responsive neurons produced
553 larger magnitude responses when incubated with TNF-FLS medium (see below). We also observed
554 that cinnamaldehyde- and menthol-evoked responses were decreased in the inflamed condition,
555 suggesting functional downregulation of TRPA1 and TRPM8, which might compensate for
556 TRPV1 sensitization with regard to overall neuron excitability. Functional downregulation of
557 TRPA1 might be explained through desensitization via increased TRPV1 function (see below) [2]
558 or via an increase in intracellular [Ca^{2+}] (due to increased excitability in the inflamed condition)
559 [63]. The latter reason can also be applied to explain decrease of menthol-evoked responses [52].

560 We also observed a tendency of a more depolarized RMP and an enhanced magnitude of capsaicin-
561 evoked peak current density of knee neurons in "inflamed" conditions, albeit both only reached
562 statistical significance in the TNF-FLS media incubated group when compared to mono-culture
563 and neuron/control FLS. However, we did not observe a decrease in the threshold of AP firing in
564 the inflamed group, despite an increased proportion of these neurons firing spontaneously, thus
565 suggesting perhaps differential susceptibility of certain knee neuron subgroups to TNF-FLS
566 mediated sensitization. For example, a secreted factor may cause one neuronal subpopulation to
567 fire spontaneously (i.e. an AP threshold of 0 pA), but overall the average AP threshold would not
568 change due to other neuronal subgroups with a higher threshold not being susceptible to

569 modulation by that secreted factor. Taken together, our data suggest soluble mediators released by
570 FLS are key players in modulating knee neuron excitability, although cell contact with FLS might
571 also play a role in sensitization. We were unable to compare the relative contributions of cell
572 contact and soluble mediators to sensitization because, in this set-up TNF-FLS is always
573 accompanied by TNF-FLS media. We posit that because our experimental design involved a media
574 change 24-hours after TNF incubation of FLS (so as not to directly stimulate neurons with residual
575 TNF-α [18]) in the neuron/TNF-FLS co-culture condition, the accumulated soluble mediator
576 concentrations were lower compared to when knee neurons were incubated in 48-hours TNF-FLS
577 conditioned media (no remaining TNF-α was measured in the media at this point). This decrease
578 in concentration of TNF-α is hypothesized to be because of FLS's inability to endogenously
579 secrete TNF-α and/or due to protein degradation [38]. Our data is consistent with a previous study
580 in FLS cells that measured TNF-α as <4 ng/ml 48-hours after stimulation with 10 ng/ml [38].
581 Similarly, in another non-TNF-α secreting cell line (Clara cells, from airways) 24-hours after
582 initial stimulation with 20 ng/ml TNF-α, the remaining concentration of TNF-α fell below the
583 detection level of the antibody array used [22].

584 Indeed, we have recently established the role of soluble mediators present in OA synovial fluid in
585 increasing neuronal excitability and TRPV1 function [12]. These soluble mediators mainly consist
586 of cytokines/chemokines which form complex signalling pathways with neurons (reviewed in
587 [43,54]). In this study, we have identified several of them to be upregulated in TNF-FLS media
588 which have been reported to be able to directly signal to neurons: IL-6 [23], KC [10], RANTES
589 [46], GM-CSF [21], LIX [42], SDF-1 [46], MCP-1 [33], and MIP-1γ (present study). In the case
590 of IL-6, MCP-1 and GM-CSF there have also been reports of an increase in TRPV1 function
591 [21,23,33].

592 In summary, we have established a co-culture system to provide evidence for a direct
593 inflammation-pain axis through FLS and DRG neurons. In the future, it can be adapted to
594 investigate FLS-mediated peripheral sensitization using FLS obtained from chronic models of
595 arthritis, activated by other pro-inflammatory cytokines or arthritic synovial fluid.

596

597 **Acknowledgements:**

598 The authors thank Dr Dora Lopresto (Department of Pharmacology, University of Cambridge) for
599 technical help with cell staining and Drs Lucy Durham and Peter Earnshaw for collection and
600 processing of human FLS samples.

601 Conflict of interests: The authors declare no competing interests.

602 Research Funding: This study was supported by Versus Arthritis Project Grants (RG 20930 and
603 RG 21973), a Rosetrees grant (M818) to E. St. J. S. and G.C., Crohn's and Colitis UK grant to
604 D.C.B. (PC2019/1-Bulmer), and a King's Together Award to L.S.T. and F.D. S.C. and C.N.B
605 were supported by Gates Cambridge Trust scholarships. L.A.P. was supported by the University
606 of Cambridge BBSRC Doctoral Training Programme (BB/M011194/1). S.L. was supported by
607 Versus Arthritis (21139).

608

609 Availability of data and materials:

610 The datasets supporting the conclusions of this article will be available in University of Cambridge
611 Apollo Repository (https://doi.org/10.17863/CAM.44367).

612

613

614 References:

615 [1] Ai R, Hammaker D, Boyle DL, Morgan R, Walsh AM, Fan S, Firestein GS, Wang W.
616 Joint-specific DNA methylation and transcriptome signatures in rheumatoid arthritis
617 identify distinct pathogenic processes. Nat Commun 2016;7:11849–11849.

618 [2] Akopian AN, Ruparel NB, Jeske NA, Hargreaves KM. Transient receptor potential
619 TRPA1 channel desensitization in sensory neurons is agonist dependent and regulated by
620 TRPV1-directed internalization. J Physiol 2007;583:175–193.

621 [3] Andersson SE, Lexmuller K, Johansson A, Ekstrom GM. Tissue and intracellular pH in
622 normal periarticular soft tissue and during different phases of antigen induced arthritis in
623 the rat. J Rheumatol 1999;26:2018–2024.

624 [4] von Banchet GS, Richter J, Hückel M, Rose C, Bräuer R, Schaible H-G. Fibroblast-like
625 synovial cells from normal and inflamed knee joints differently affect the expression of
626 pain-related receptors in sensory neurones: a co-culture study. Arthritis Research &
627 Therapy 2007;9:R6–R6.

628 [5] Bartok B, Firestein GS. Fibroblast-like synoviocytes: key effector cells in rheumatoid
629 arthritis. Immunological reviews 2010;233:233–255.

630 [6] Blue ML, Conrad P, Webb DL, Sarr T, Macaro M. Interacting monocytes and
631 synoviocytes induce adhesion molecules by a cytokine-regulated process. Lymphokine
632 Cytokine Res 1993;12:213–218.

633 [7] Bombara MR, Webb DL, Conrad P, Marior CW, Sarr T, Ranges GE, Aune TM, Grave
634 JM, Blue M-L. Cell contact between T cells and synovial fibroblasts causes induction of
635 adhesion molecules and cytokines. Journal of Leukocyte Biology 1993;54:399–406.

636 [8] Bondeson J, Wainwright SD, Lauder S, Amos N, Hughes CE. The role of synovial
637 macrophages and macrophage-produced cytokines in driving aggrecanases, matrix
638 metalloproteinases, and other destructive and inflammatory responses in osteoarthritis.
639 Arthritis Research & Therapy 2006;8:R187.

640 [9] Bottini N, Firestein GS. Duality of fibroblast-like synoviocytes in RA: passive responders
641 and imprinted aggressors. Nat Rev Rheumatol 2013;9. doi:10.1038/nrrheum.2012.190.

642 [10] Brandolini L, Benedetti E, Ruffini PA, Russo R, Cristiano L, Antonosante A, d'Angelo M,
643 Castelli V, Giordano A, Allegretti M, Cimini A. CXCR1/2 pathways in paclitaxel-induced
644 neuropathic pain. Oncotarget 2017;8:23188–23201.

645 [11] Burger D, Rezzonico R, Li J-M, Modoux C, Pierce RA, Welgus HG, Dayer J-M.
646 Imbalance between interstitial collagenase and tissue inhibitor of metalloproteinases 1 in
647 synoviocytes and fibroblasts upon direct contact with stimulated T lymphocytes:

648 Involvement of membrane-associated cytokines. Arthritis & Rheumatism 1998;41:1748–
649 1759.

650 [12] Chakrabarti S, Jadon DR, Bulmer DC, Smith EStJ. Human osteoarthritic synovial fluid
651 increases excitability of mouse dorsal root ganglion sensory neurons: an in-vitro
652 translational model to study arthritic pain. Rheumatology 2019.
653 doi:10.1093/rheumatology/kez331.

654 [13] Chakrabarti S, Pattison LA, Singhal K, Hockley JRF, Callejo G, Smith EStJ. Acute
655 inflammation sensitizes knee-innervating sensory neurons and decreases mouse digging
656 behavior in a TRPV1-dependent manner. Neuropharmacology 2018;143:49–62.

657 [14] Chen C-X, Chen J-Y, Kou J-Q, Xu Y-L, Wang S-Z, Zhu Q, Yang L, Qin Z-H.
658 Suppression of Inflammation and Arthritis by Orally Administrated Cardiotoxin from Naja
659 naja atra. Evid Based Complement Alternat Med 2015;2015:387094.

660 [15] Chomarat P, Rissoan MC, Pin JJ, Banchereau J, Miossec P. Contribution of IL-1, CD14,
661 and CD13 in the increased IL-6 production induced by in vitro monocyte-synoviocyte
662 interactions. J Immunol 1995;155:3645.

663 [16] Clark RB, Schmidt TA, Sachse FB, Boyle D, Firestein GS, Giles WR. Cellular
664 electrophysiological principles that modulate secretion from synovial fibroblasts. J Physiol
665 2017;595:635–645.

666 [17] Croft AP, Campos J, Jansen K, Turner JD, Marshall J, Attar M, Savary L, Wehmeyer C,
667 Naylor AJ, Kemble S, Begum J, Dürholz K, Perlman H, Barone F, McGettrick HM,
668 Fearon DT, Wei K, Raychaudhuri S, Korsunsky I, Brenner MB, Coles M, Sansom SN,
669 Filer A, Buckley CD. Distinct fibroblast subsets drive inflammation and damage in
670 arthritis. Nature 2019;570:246–251.

671 [18] Czeschik JC, Hagenacker T, Schäfers M, Büsselberg D. TNF-α differentially modulates
672 ion channels of nociceptive neurons. Neuroscience Letters 2008;434:293–298.

673 [19] Dawes JM, Kiesewetter H, Perkins JR, Bennett DLH, McMahon SB. Chemokine
674 expression in peripheral tissues from the monosodium iodoacetate model of chronic joint
675 pain. Mol Pain 2013;9:57–57.

676 [20] Dittert I, Benedikt J, Vyklický L, Zimmermann K, Reeh PW, Vlachová V. Improved
677 superfusion technique for rapid cooling or heating of cultured cells under patch-clamp
678 conditions. Journal of Neuroscience Methods 2006;151:178–185.

679 [21] Donatien P, Anand U, Yiangou Y, Sinisi M, Fox M, MacQuillan A, Quick T, Korchev
680 YE, Anand P. Granulocyte-macrophage colony-stimulating factor receptor expression in
681 clinical pain disorder tissues and role in neuronal sensitization. Pain Rep 2018;3:e676–
682 e676.

683 [22] Elizur A, Adair-Kirk TL, Kelley DG, Griffin GL, Demello DE, Senior RM. Tumor
684 necrosis factor-alpha from macrophages enhances LPS-induced clara cell expression of
685 keratinocyte-derived chemokine. Am J Respir Cell Mol Biol 2008;38:8–15.

686 [23] Fang D, Kong L-Y, Cai J, Li S, Liu X-D, Han J-S, Xing G-G. Interleukin-6-mediated
687 functional upregulation of TRPV1 receptors in dorsal root ganglion neurons through the
688 activation of JAK/PI3K signaling pathway: roles in the development of bone cancer pain
689 in a rat model. Pain 2015;156:1124–1144.

690 [24] Farr M, Garvey K, Bold AM, Kendall MJ, Bacon PA. Significance of the hydrogen ion
691 concentration in synovial fluid in rheumatoid arthritis. Clin Exp Rheumatol 1985;3:99–
692 104.

693 [25] Futami I, Ishijima M, Kaneko H, Tsuji K, Ichikawa-Tomikawa N, Sadatsuki R, Muneta T,
694 Arikawa-Hirasawa E, Sekiya I, Kaneko K. Isolation and Characterization of
695 Multipotential Mesenchymal Cells from the Mouse Synovium. PLoS ONE
696 2012;7:e45517.

697 [26] Gong W, Kolker SJ, Usachev Y, Walder RY, Boyle DL, Firestein GS, Sluka KA. Acid-
698 sensing ion channel 3 decreases phosphorylation of extracellular signal-regulated kinases
699 and induces synoviocyte cell death by increasing intracellular calcium. Arthritis Research
700 & Therapy 2014;16:R121.

701 [27] Guo W, Yu D, Wang X, Luo C, Chen Y, Lei W, Wang C, Ge Y, Xue W, Tian Q, Gao X,
702 Yao W. Anti-inflammatory effects of interleukin-23 receptor cytokine-binding homology
703 region rebalance T cell distribution in rodent collagen-induced arthritis. Oncotarget
704 2016;7:31800–31813.

705 [28] Hannan MT. Epidemiologic perspectives on women and arthritis: An overview. Arthritis
706 & Rheumatism 1996;9:424–434.

707 [29] Hardy RS, Hülso C, Liu Y, Gasparini SJ, Fong-Yee C, Tu J, Stoner S, Stewart PM, Raza
708 K, Cooper MS, Seibel MJ, Zhou H. Characterisation of fibroblast-like synoviocytes from a
709 murine model of joint inflammation. Arthritis Research & Therapy 2013;15:R24–R24.

710 [30] Hong R, Sur B, Yeom M, Lee B, Kim KS, Rodriguez JP, Lee S, Kang KS, Huh C-K, Lee
711 SC, Hahm D-H. Anti-inflammatory and anti-arthritic effects of the ethanolic extract of
712 Aralia continentalis Kitag. in IL-1β-stimulated human fibroblast-like synoviocytes and
713 rodent models of polyarthritis and nociception. Phytomedicine 2018;38:45–56.

714 [31] Ita ME, Winkelstein BA. Concentration-Dependent Effects of Fibroblast-Like
715 Synoviocytes on Collagen Gel Multiscale Biomechanics and Neuronal Signaling:
716 Implications for Modeling Human Ligamentous Tissues. Journal of Biomechanical
717 Engineering 2019;141. doi:10.1115/1.4044051.

718 [32] Jones DS, Jenney AP, Swantek JL, Burke JM, Lauffenburger DA, Sorger PK. Profiling
719 drugs for rheumatoid arthritis that inhibit synovial fibroblast activation. Nature Chemical
720 Biology 2016;13:38.

721 [33] Jung H, Toth PT, White FA, Miller RJ. Monocyte chemoattractant protein-1 functions as a
722 neuromodulator in dorsal root ganglia neurons. J Neurochem 2008;104:254–263.

723 [34] Kawashima M, Ogura N, Akutsu M, Ito K, Kondoh T. The anti-inflammatory effect of
724 cyclooxygenase inhibitors in fibroblast-like synoviocytes from the human
725 temporomandibular joint results from the suppression of PGE2 production. Journal of oral
726 pathology & medicine : official publication of the International Association of Oral
727 Pathologists and the American Academy of Oral Pathology 2013;42:499–506.

728 [35] Kochukov MY, McNearney TA, Yin H, Zhang L, Ma F, Ponomareva L, Abshire S,
729 Westlund KN. Tumor Necrosis Factor-Alpha (TNF-α) Enhances Functional Thermal and
730 Chemical Responses of TRP Cation Channels in Human Synoviocytes. Mol Pain
731 2009;5:1744-8069-5–49.

732 [36] Larsson S, Englund M, Struglics A, Lohmander LS. Interleukin-6 and tumor necrosis
733 factor alpha in synovial fluid are associated with progression of radiographic knee
734 osteoarthritis in subjects with previous meniscectomy. Osteoarthritis and Cartilage
735 2015;23:1906–1914.

736 [37] Lebre MC, Vieira PL, Tang MW, Aarrass S, Helder B, Newsom-Davis T, Tak PP,
737 Screaton GR. Synovial IL-21/TNF-producing CD4+ T cells induce joint destruction in
738 rheumatoid arthritis by inducing matrix metalloproteinase production by fibroblast-like
739 synoviocytes. Journal of Leukocyte Biology 2017;101:775–783.

740 [38] Lee A, Qiao Y, Grigoriev G, Chen J, Park-Min K-H, Park SH, Ivashkiv LB, Kalliolias
741 GD. Tumor necrosis factor α induces sustained signaling and a prolonged and unremitting
742 inflammatory response in rheumatoid arthritis synovial fibroblasts. Arthritis Rheum
743 2013;65:928–938.

744 [39] Livak KJ, Schmittgen TD. Analysis of Relative Gene Expression Data Using Real-Time
745 Quantitative PCR and the 2−ΔΔCT Method. Methods 2001;25:402–408.

746 [40] Llop-Guevara A, Porras M, Cendón C, Di Ceglie I, Siracusa F, Madarena F, Rinotas V,
747 Gómez L, van Lent PL, Douni E, Chang HD, Kamradt T, Román J. Simultaneous
748 inhibition of JAK and SYK kinases ameliorates chronic and destructive arthritis in mice.
749 Arthritis Research & Therapy 2015;17:356.

750 [41] McCall MN, McMurray HR, Land H, Almudevar A. On non-detects in qPCR data.
751 Bioinformatics 2014;30:2310–2316.

752 [42] Merabova N, Kaminski R, Krynska B, Amini S, Khalili K, Darbinyan A. JCV
753 agnoprotein-induced reduction in CXCL5/LIX secretion by oligodendrocytes is associated
754 with activation of apoptotic signaling in neurons. J Cell Physiol 2012;227:3119–3127.

755 [43] Miller RJ, Jung H, Bhangoo SK, White FA. Cytokine and chemokine regulation of
756 sensory neuron function. Handb Exp Pharmacol 2009:417–449.

757 [44] Neumann E, Lefèvre S, Zimmermann B, Gay S, Müller-Ladner U. Rheumatoid arthritis
758 progression mediated by activated synovial fibroblasts. Trends in Molecular Medicine
759 2010;16:458–468.

760 [45] Noss EH, Brenner MB. The role and therapeutic implications of fibroblast-like
761 synoviocytes in inflammation and cartilage erosion in rheumatoid arthritis. Immunological
762 Reviews 2008;223:252–270.

763 [46] Oh SB, Tran PB, Gillard SE, Hurley RW, Hammond DL, Miller RJ. Chemokines and
764 Glycoprotein120 Produce Pain Hypersensitivity by Directly Exciting Primary Nociceptive
765 Neurons. J Neurosci 2001;21:5027.

766 [47] Parsonage G, Falciani F, Burman A, Filer A, Ross E, Bofill M, Martin S, Salmon M,
767 Buckley CD. Global gene expression profiles in fibroblasts from synovial, skin and
768 lymphoid tissue reveals distinct cytokine and chemokine expression patterns. Thromb
769 Haemost 2017;90:688–697.

770 [48] Picelli S, Faridani OR, Björklund ÅK, Winberg G, Sagasser S, Sandberg R. Full-length
771 RNA-seq from single cells using Smart-seq2. Nature Protocols 2014;9:171–181.

772 [49] Rojewska E, Zychowska M, Piotrowska A, Kreiner G, Nalepa I, Mika J. Involvement of
773 Macrophage Inflammatory Protein-1 Family Members in the Development of Diabetic
774 Neuropathy and Their Contribution to Effectiveness of Morphine. Front Immunol
775 2018;9:494–494.

776 [50] Rosengren S, Boyle DL, Firestein GS. Acquisition, culture, and phenotyping of synovial
777 fibroblasts. Methods in molecular medicine 2007;135:365–375.

778 [51] Safiri S, Kolahi AA, Hoy D, Smith E, Bettampadi D, Mansournia MA, Almasi-Hashiani
779 A, Ashrafi-Asgarabad A, Moradi-Lakeh M, Qorbani M, Collins G, Woolf AD, March L,
780 Cross M. Global, regional and national burden of rheumatoid arthritis 1990–2017: a
781 systematic analysis of the Global Burden of Disease study 2017. Ann Rheum Dis
782 2019;78:1463.

783 [52] Sarria I, Ling J, Zhu MX, Gu JG. TRPM8 acute desensitization is mediated by calmodulin
784 and requires PIP(2): distinction from tachyphylaxis. J Neurophysiol 2011;106:3056–3066.

785 [53] Saxne T, Palladino Jr MA, Heinegãrd D, Talal N, Wollheim FA. Detection of tumor
786 necrosis factor α but not tumor necrosis factor β in rheumatoid arthritis synovial fluid and
787 serum. Arthritis & Rheumatism 1988;31:1041–1045.

788 [54] Schaible H-G. Nociceptive neurons detect cytokines in arthritis. ARTHRITIS
789 RESEARCH & THERAPY 2014;16.

790 [55] Scott BB, Weisbrot LM, Greenwood JD, Bogoch ER, Paige CJ, Keystone EC.
791 Rheumatoid arthritis synovial fibroblast and U937 macrophage/monocyte cell line
792 interaction in cartilage degradation. Arthritis & Rheumatism 1997;40:490–498.

793 [56] Sluka KA, Rasmussen LA, Edgar MM, O'Donnell JM, Walder RY, Kolker SJ, Boyle DL,
794 Firestein GS. Acid-sensing ion channel 3 deficiency increases inflammation but decreases
795 pain behavior in murine arthritis. 2013.

796 [57] Stefanini M, Martino C de, Zamboni L. Fixation of Ejaculated Spermatozoa for Electron
797 Microscopy. Nature 1967;216:173–174.

798 [58] Syx D, Tran PB, Miller RE, Malfait A-M. Peripheral Mechanisms Contributing to
799 Osteoarthritis Pain. Current Rheumatology Reports 2018;20:9.

800 [59] Taciak B, Białasek M, Braniewska A, Sas Z, Sawicka P, Kiraga Ł, Rygiel T, Król M.
801 Evaluation of phenotypic and functional stability of RAW 264.7 cell line through serial
802 passages. PLOS ONE 2018;13:e0198943.

803 [60] Taylor PC, Feldmann M. Anti-TNF biologic agents: still the therapy of choice for
804 rheumatoid arthritis. Nature Reviews Rheumatology 2009;5:578.

805 [61] Tetta C, Camussi G, Modena V, Di Vittorio C, Baglioni C. Tumour necrosis factor in
806 serum and synovial fluid of patients with active and severe rheumatoid arthritis. Ann
807 Rheum Dis 1990;49:665–667.

808 [62] van Vollenhoven RF. Sex differences in rheumatoid arthritis: more than meets the eye..
809 BMC Med 2009;7:12–12.

810 [63] Wang YY, Chang RB, Waters HN, McKemy DD, Liman ER. The nociceptor ion channel
811 TRPA1 is potentiated and inactivated by permeating calcium ions. J Biol Chem
812 2008;283:32691–32703.

813 [64] Westlund KN, Kochukov MY, Lu Y, McNearney TA. Impact of Central and Peripheral
814 TRPV1 and ROS Levels on Proinflammatory Mediators and Nociceptive Behavior. Mol
815 Pain 2010;6:1744-8069-6–46.

816 [65] Woolf CJ, Allchorne A, Safieh-Garabedian B, Poole S. Cytokines, nerve growth factor
817 and inflammatory hyperalgesia: the contribution of tumour necrosis factor α. British
818 Journal of Pharmacology 1997;121:417–424.

819 [66] Wright AJ, Husson ZMA, Hu D-E, Callejo G, Brindle KM, Smith EStJ. Increased
820 hyperpolarized [1-13C] lactate production in a model of joint inflammation is not
821 accompanied by tissue acidosis as assessed using hyperpolarized 13C-labelled
822 bicarbonate. NMR in Biomedicine 2018:e3892-n/a.

823 [67] Yamamura Y, Gupta R, Morita Y, He X, Pai R, Endres J, Freiberg A, Chung K, Fox DA.
824 Effector Function of Resting T Cells: Activation of Synovial Fibroblasts. J Immunol
825 2001;166:2270.

826 [68] Zhang F, Wei K, Slowikowski K, Fonseka CY, Rao DA, Kelly S, Goodman SM,
827 Tabechian D, Hughes LB, Salomon-Escoto K, Watts GFM, Jonsson AH, Rangel-Moreno
828 J, Meednu N, Rozo C, Apruzzese W, Eisenhaure TM, Lieb DJ, Boyle DL, Mandelin AM

829 2nd, Accelerating Medicines Partnership Rheumatoid Arthritis and Systemic Lupus
830 Erythematosus (AMP RA/SLE) Consortium, Boyce BF, DiCarlo E, Gravallese EM,
831 Gregersen PK, Moreland L, Firestein GS, Hacohen N, Nusbaum C, Lederer JA, Perlman
832 H, Pitzalis C, Filer A, Holers VM, Bykerk VP, Donlin LT, Anolik JH, Brenner MB,
833 Raychaudhuri S. Defining inflammatory cell states in rheumatoid arthritis joint synovial
834 tissues by integrating single-cell transcriptomics and mass cytometry. Nat Immunol
835 2019;20:928–942.

836

837 Figure Legends:

838 Figure 1: Induction of inflammation in FLS derived from mouse knee.

839 A) Representative picture showing exposed inside of the patella (black triangle) and the
840 surrounding ligament and fat pad (white triangle) after midline resection and distal pull of the
841 quadriceps muscles. Scale bar = 2 mm. B) Representative picture of FLS in culture. Scale bar =
842 50 µm. C) Bars represent fold change of the genes *Il-6*, *Il-1r1*, *Cox-2* and *Cox-1* from either Contra
843 (vs. Ipsi) or control (vs. TNF). Black hatched bars = control FLS, red bars = TNF-FLS, grey bar =
844 Contra, white bar = Ipsi. All FLS at P5. D) Images of mouse inflammatory array membranes
845 probed against FLS conditioned medium (i) which were quantified by densitometry and
846 represented as bar graphs showing fold change of various cytokines between control and TNF-
847 FLS (ii, multiple t-test with Holm-Sidak correction) and among Contra, Ipsi and TNF from control
848 FLS media (iii, ANOVA with Tukey's post-hoc test) and spot intensity differences. Dotted
849 rectangles highlight IL-6 spots (Di) and corresponding quantifications (Dii, iii). Only cytokines
850 that were present in all of the compared groups are shown in graphs. * $p < 0.05$, ** $p < 0.01$, ***
851 $p < 0.001$ and **** $p < 0.0001$. Error bars = SEM.

852

853 Figure 2. Pro-inflammatory gene expression in FLS derived from arthritic human patients.

854 A) Transcripts per million values of selected inflammatory markers extracted from RNA-Seq data
855 of human FLS from RA and OA donors [68]. Results reveal detectable levels of the pro-
856 inflammatory genes *IL-6*, *IL-8*, *IL-1R1*, *KC*, *MCP-1*, *SDF-1* and *Fractalkine* in FLS from both OA
857 (black) and RA (blue) patients. *LIX* was considered undetectable as the mean transcript per million
858 value was below the threshold of 1. B) Bar graphs showing fold change in expression levels
859 (determined by qPCR) of *IL-6, KC, LIX, MCP-1, IL-8, IL-1R1, SDF-1* and *Fractalkine* in control
860 vs. TNF-α stimulated FLS derived from human RA (filled circles) and OA (open circles) patients
861 (n = 4). * $p < 0.05$, ** $p < 0.01$, unpaired t-test.

862

863

864 Figure 3: Murine TNF-FLS mediated increase in excitability of knee neurons.

865 A) Representative live-cell imaging picture showing FLS (magenta) and neuron (cyan) in co-
866 culture. Scale bar = 50 µm. B) Representative FB labelled knee neuron (white arrow) being
867 recorded using a patch pipette (triangular shadow), surrounded by FLS (yellow arrow). Scale bar
868 = 50 µm. C) Pie-chart showing proportion of knee neurons that fired AP without current
869 stimulation in healthy (neuron mono-culture + neuron/control FLS, n = 37, black) and inflamed
870 (neuron/TNF-FLS + neuron/TNF-FLS media, n = 41, red) condition. D) Representative knee
871 neuron incubated with TNF-FLS media firing spontaneous AP along with schematic diagram of
872 AP properties measured (inset). E) Bar graphs showing measured RMP (i), threshold (ii), AHP
873 peak (iii) and HPD (iv) from knee neurons in mono-culture (n = 19, white bar/black open circle),
874 in co-culture with control FLS (n = 18, grey bar/black dotted circle), in co-culture with TNF-FLS
875 (n = 20, light red bar/red dotted circle) and incubated in TNF-FLS media (n = 21, white bar/red

open circle). * $p < 0.05$ and *** $p < 0.001$, ANOVA followed by Tukey's post hoc test. Data from 4-5 female mice in each group. Error bars = SEM.

Figure 4: Murine TNF-FLS mediated modulation of TRP agonist response in knee neurons.

Representative traces showing capsaicin (TRPV1 agonist, Ai), cinnamaldehyde (TRPA1 agonist, Bi) and menthol- (TRPM8 agonist, Ci) evoked responses in knee neurons. Black traces obtained from knee neuron in mono-culture, red trace obtained from knee neuron incubated in TNF-FLS media. White boxes represent perfusion of extracellular solution. Bar graphs showing peak current densities of capsaicin- (Aii), cinnamaldehyde- (Bii) or menthol-evoked (Cii) currents from knee neurons in mono-culture (white bar/black open circle), in co-culture with control FLS (grey bar/black dotted circle), in co-culture with TNF-FLS (light red bar/red dotted circle) and incubated in TNF-FLS media (white bar/red open circle) Comparison between groups made using ANOVA with Tukey's post hoc test. Bar graphs showing percent of knee neurons that responded to capsaicin (Aiii), cinnamaldehyde (Biii) and menthol (Ciii) in healthy (neuron mono-culture + neuron/control FLS) and inflamed (neuron/TNF-FLS + neuron/TNF-FLS media) condition. Comparison made using chi-sq test. * $p < 0.05$. Data from 4-5 female mice in each group. Error bars = SEM.

Figure 1

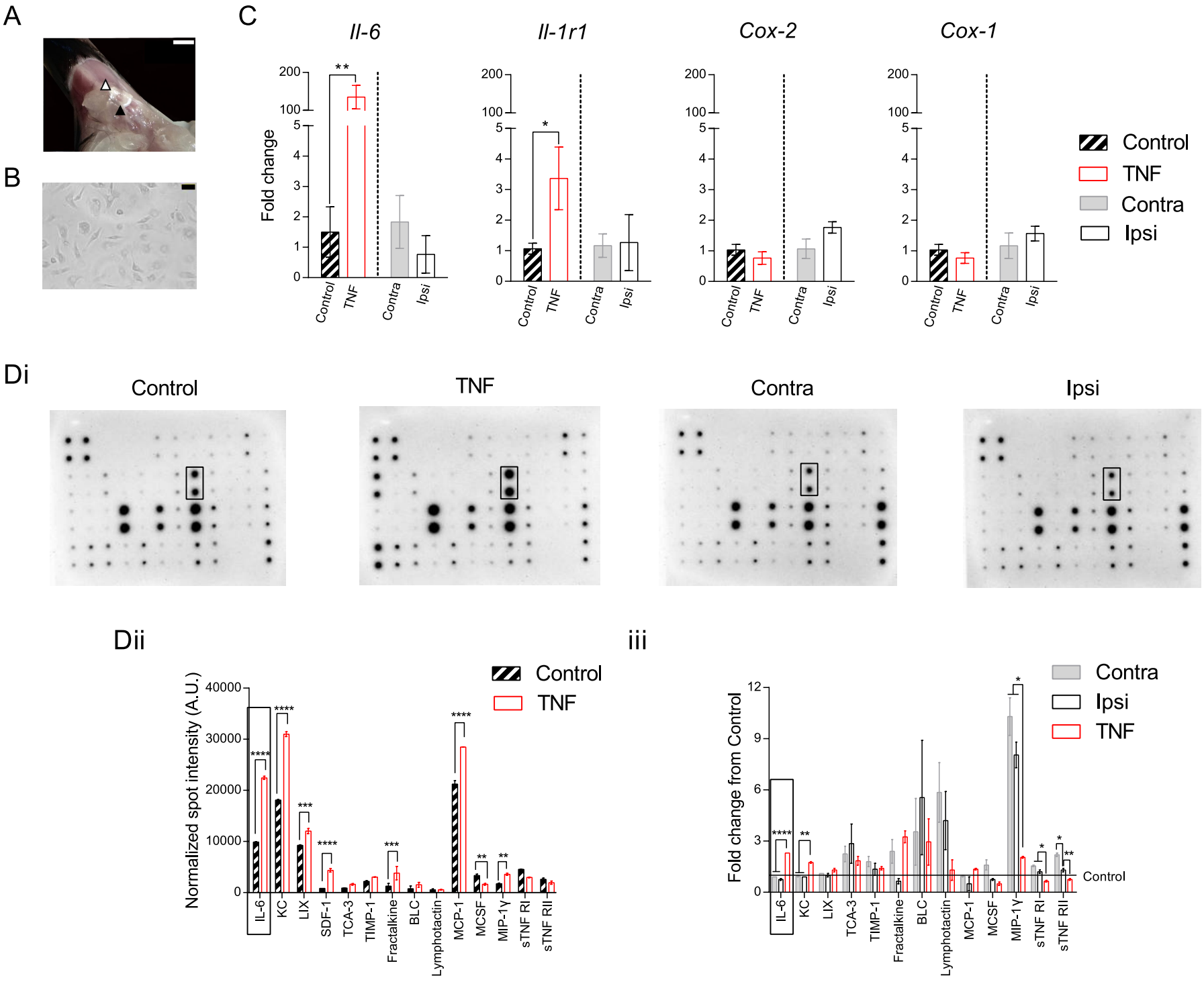
A
B
C
Il-6
Il-1r1
Cox-2
Cox-1
Fold change
Control
TNF
Contra
Ipsi
Di
Control
TNF
Contra
Ipsi
Dii
Normalized spot intensity (A.U.)
IL-6
KC
LIX
SDF-1
TCA-3
TIMP-1
Fractalkine
BLC
Lymphotactin
MCP-1
MCSF
MIP-1γ
sTNF RI
sTNF RII
iii
Fold change from Control

Figure 2

A

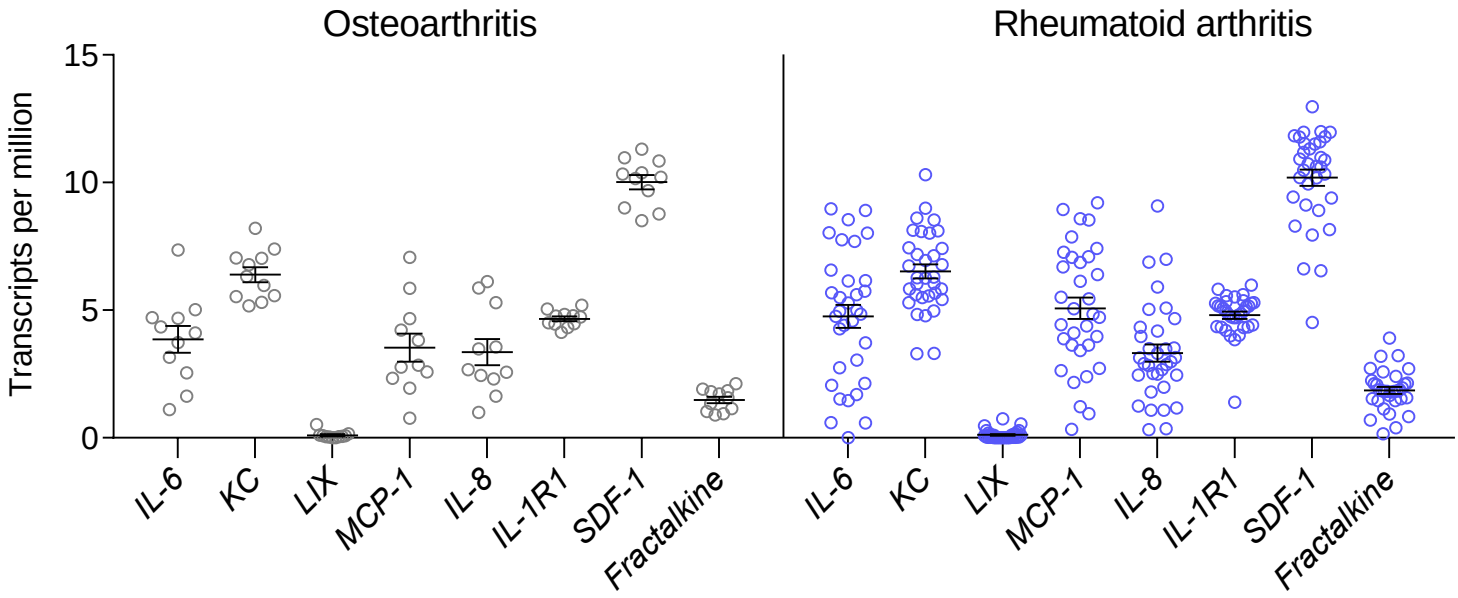
Osteoarthritis
Rheumatoid arthritis
Transcripts per million
15
10
5
0
IL-6
KC
LIX
MCP-1
IL-8
IL-1R1
SDF-1
Fractalkine

B

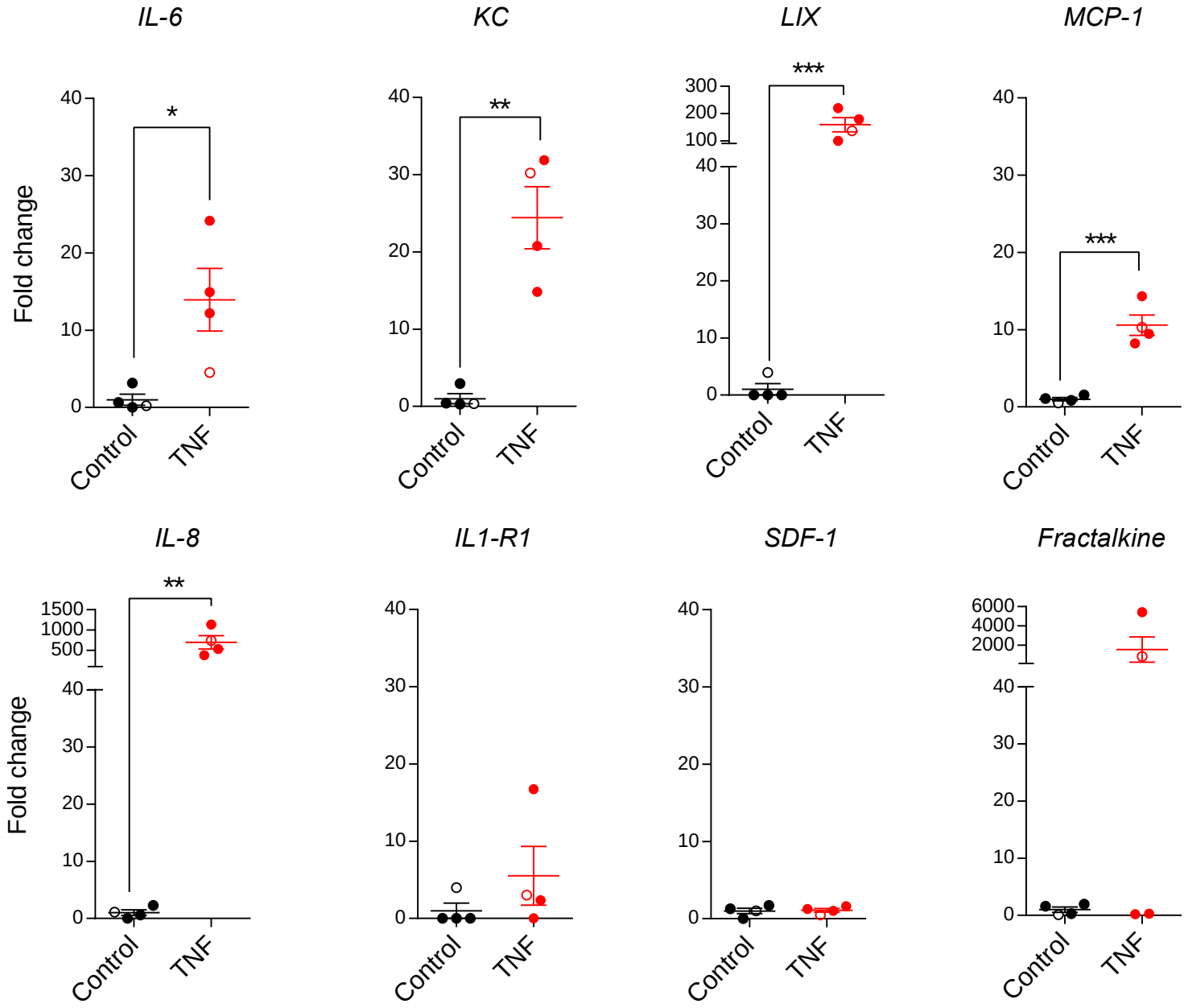
IL-6
KC
LIX
MCP-1
IL-8
IL1-R1
SDF-1
Fractalkine
Fold change
Control
TNF
*
**
***

Figure 3

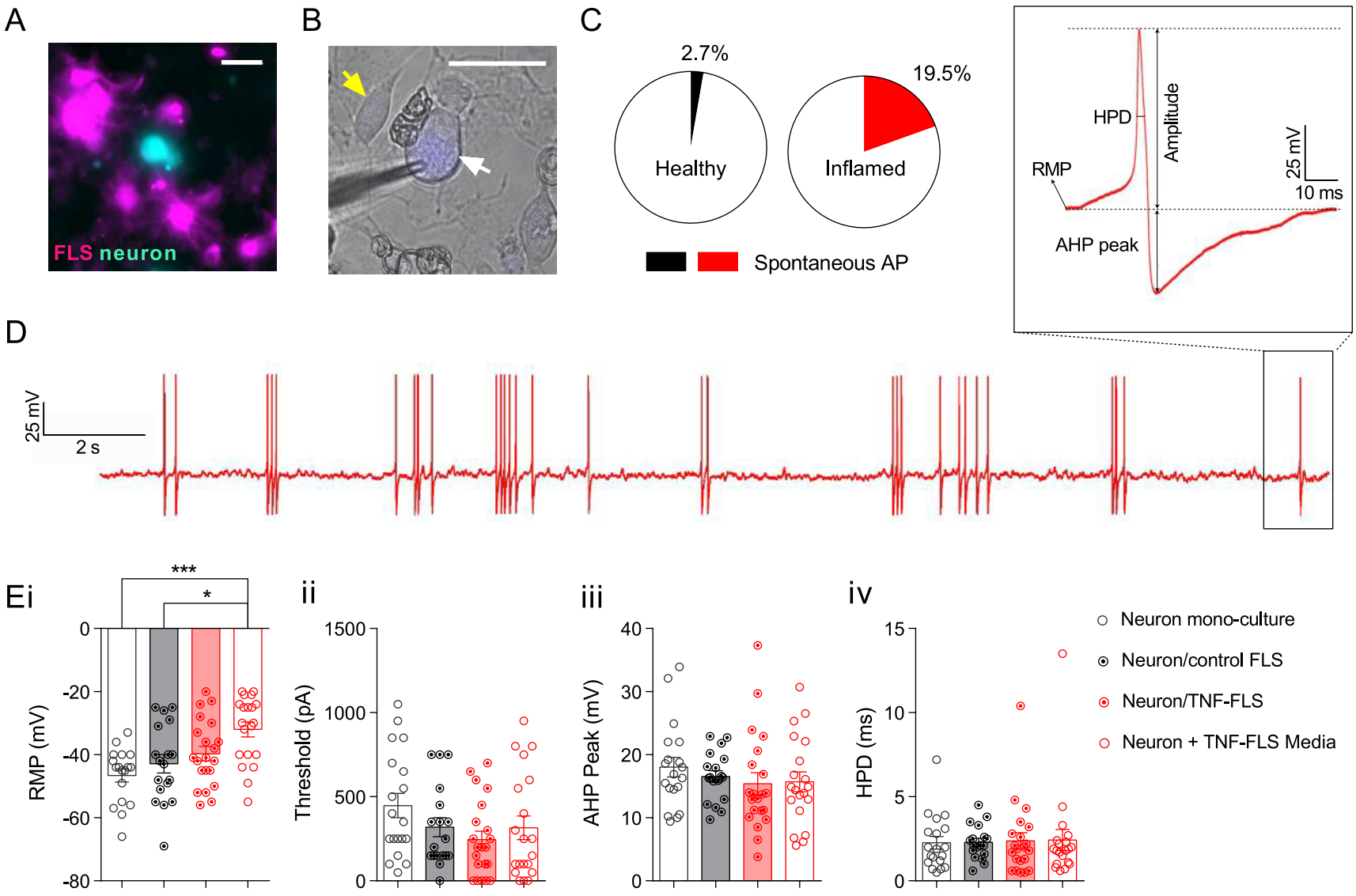
A
FLS neuron
B
C
2.7%
Healthy
19.5%
Inflamed
Spontaneous AP
HPD
Amplitude
RMP
AHP peak
25 mV
10 ms
D
25 mV
2 s
Ei
***
*
RMP (mV)
0
-20
-40
-60
-80
ii
Threshold (pA)
1500
1000
500
0
iii
AHP Peak (mV)
40
30
20
10
0
iv
HPD (ms)
15
10
5
0
Neuron mono-culture
Neuron/control FLS
Neuron/TNF-FLS
Neuron + TNF-FLS Media

Figure 4

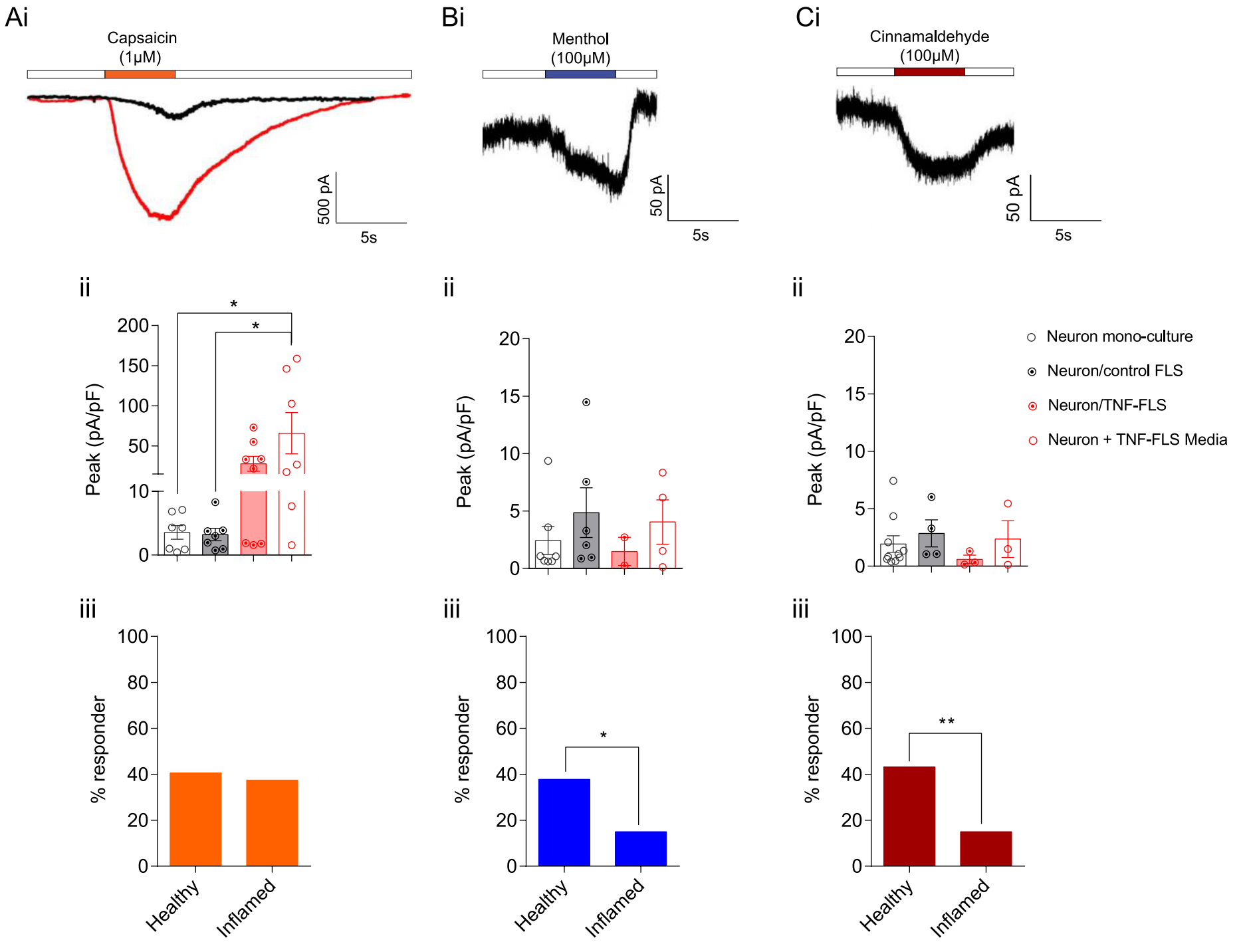
Ai
Capsaicin
(1μM)
500 pA
5s
Bi
Menthol
(100μM)
50 pA
5s
Ci
Cinnamaldehyde
(100μM)
50 pA
5s
ii
Peak (pA/pF)
200
150
100
50
10
0
*
*
ii
Peak (pA/pF)
20
15
10
5
0
ii
Peak (pA/pF)
20
15
10
5
0
Neuron mono-culture
Neuron/control FLS
Neuron/TNF-FLS
Neuron + TNF-FLS Media
iii
% responder
100
80
60
40
20
0
Healthy
Inflamed
iii
% responder
100
80
60
40
20
0
*
Healthy
Inflamed
iii
% responder
100
80
60
40
20
0
**
Healthy
Inflamed

Table 1: AP properties of knee neurons. *** represents $p < 0.001$ when compared to knee neuron mono-culture, $ represents $p < 0.05$ when compared to neuron/control FLS co-culture.

	Knee neuron mono-culture (n = 19)		Knee neuron/control FLS (n = 18)		Knee neuron/TNF-FLS (n = 21)		Knee neuron/TNF-FLS media (n = 20)	
	Mean	SEM	Mean	SEM	Mean	SEM	Mean	SEM.
RMP (mV)	-46.6	2.0	-42.8	2.9	-39.7	2.3	-32.0***/$	2.3
Threshold (pA)	447.4	71.5	319.4	56.3	245.2	49.4	315.0	70.0
Half peak duration (HPD, ms)	2.2	0.4	2.3	0.2	2.4	0.5	2.4	0.6
Afterhyperpolarization amplitude (AHP peak, mV)	13.7	2.6	19.6	2.7	16.1	2.9	21.6	3.3

Supplementary Figure 1

Characterization of FLS

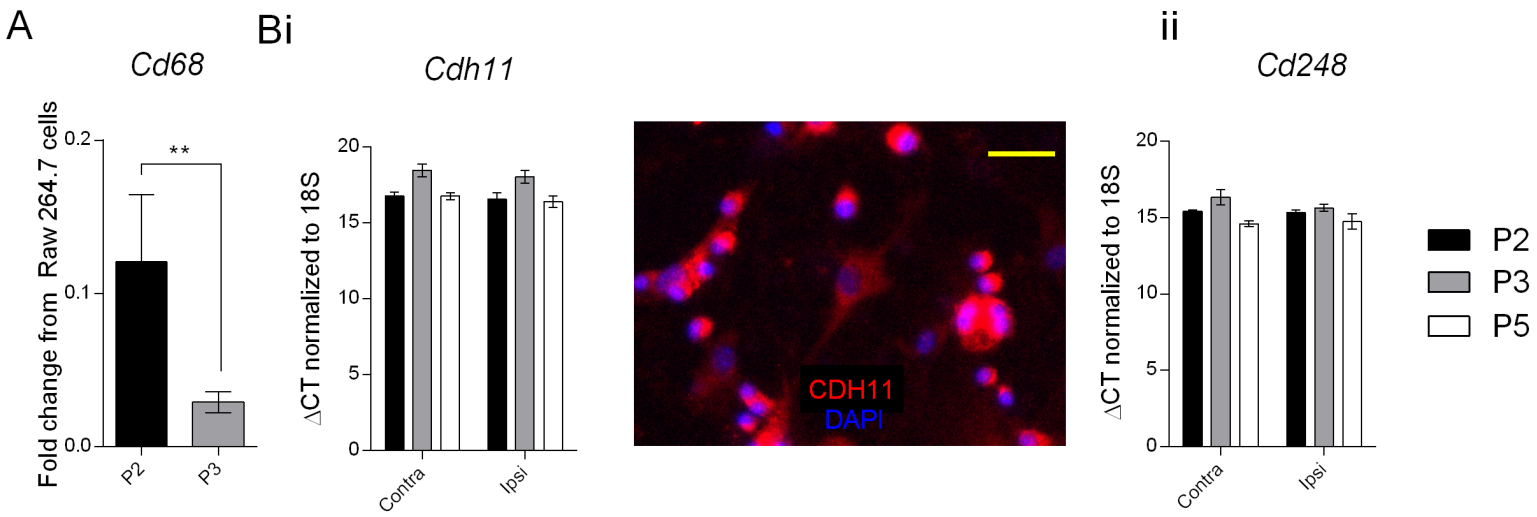

Expression of inflammation-related genes in FLS derived from CFA-injected knee joint

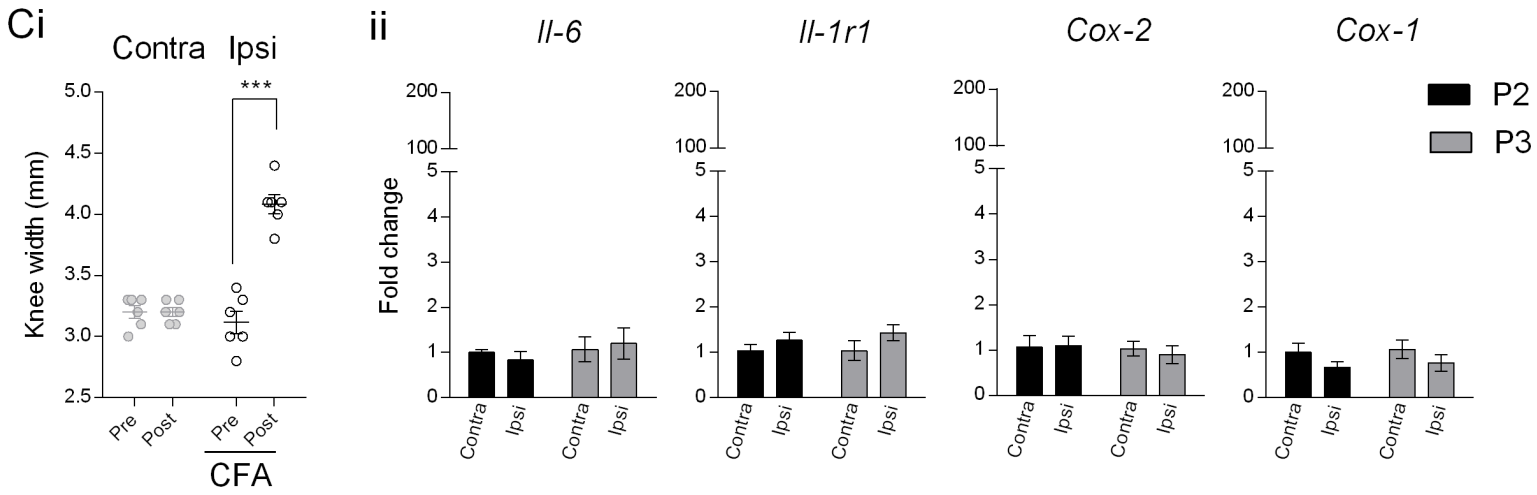

MIP-1γ activation of DRG neurons

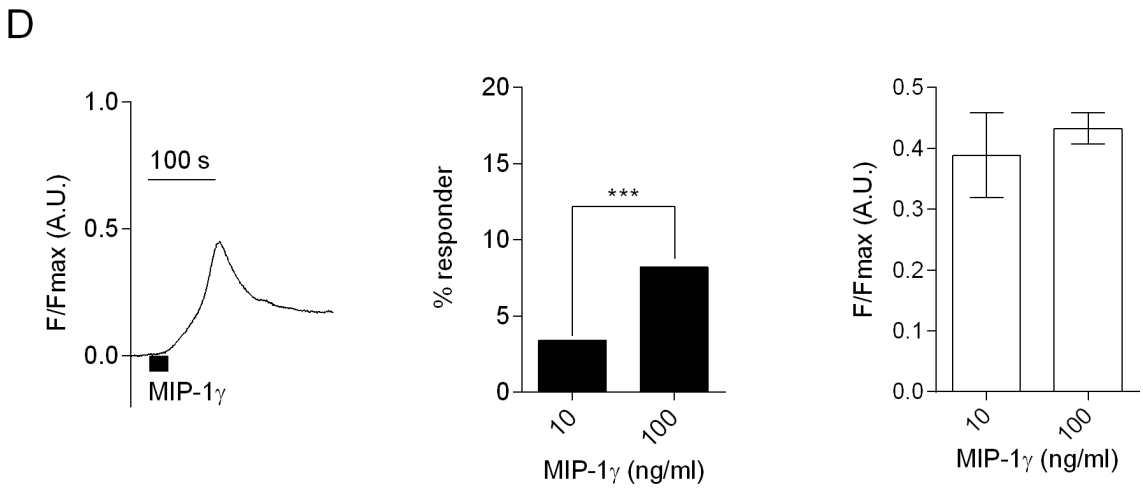

A

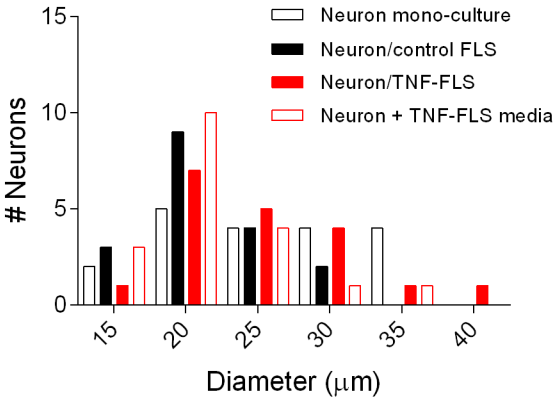

B

Small neurons (<20 μm)

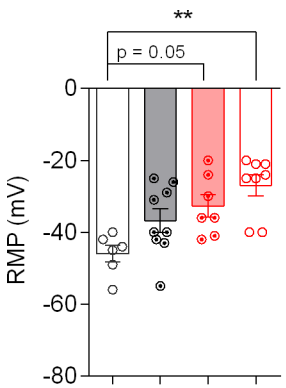

Medium - large neurons (>20 μm)

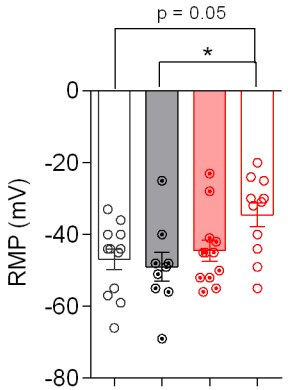

Neuron monoculture

Neuron/control FLS

Neuron/TNF-FLS

Neuron +
TNF-FLS media

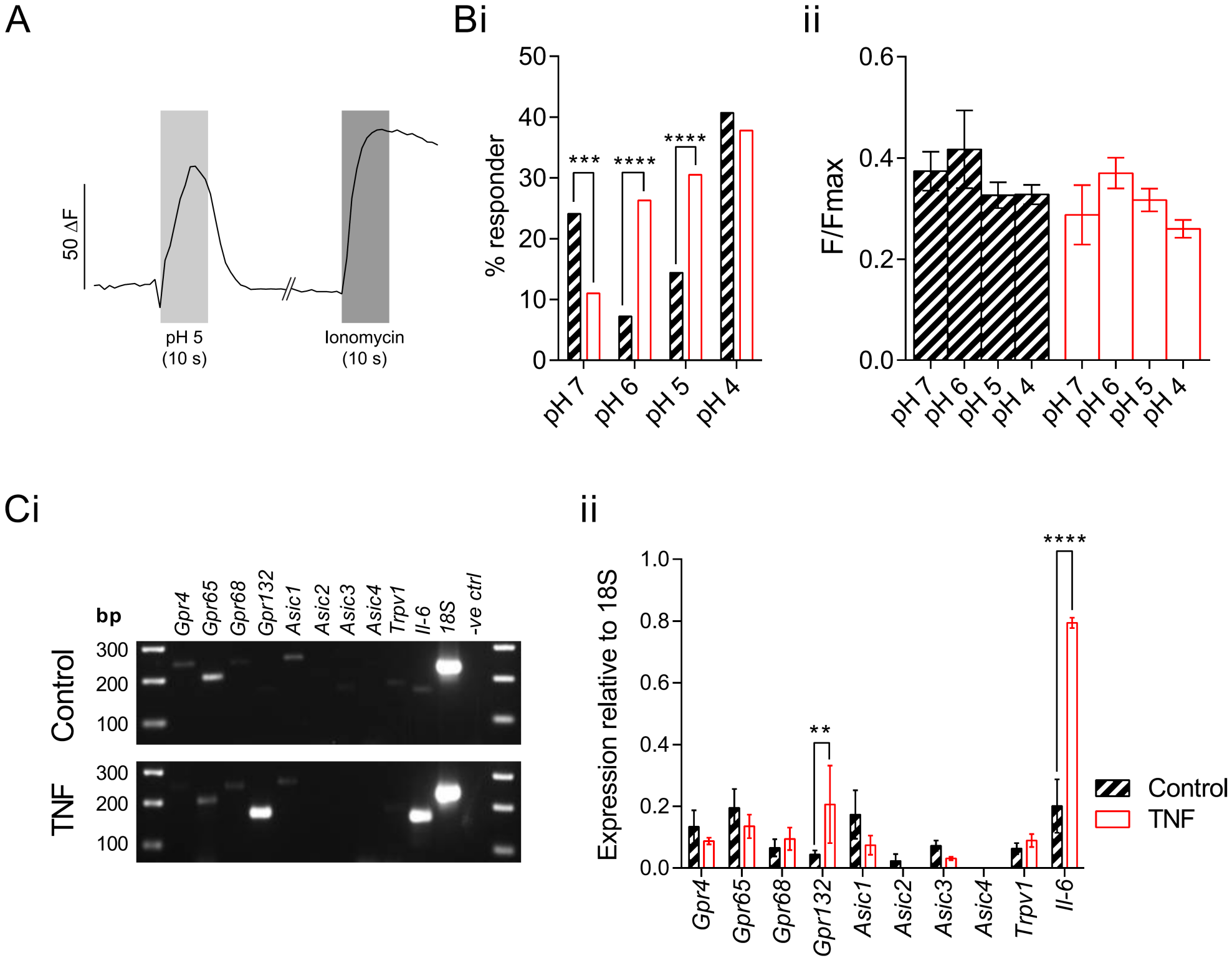
A
50 ΔF
pH 5
(10 s)
Ionomycin
(10 s)
Bi
% responder
***
****
****
pH 7
pH 6
pH 5
pH 4
ii
F/Fmax
pH 7
pH 6
pH 5
pH 4
pH 7
pH 6
pH 5
pH 4
Ci
bp
Gpr4
Gpr65
Gpr68
Gpr132
Asic1
Asic2
Asic3
Asic4
Trpv1
Il-6
18S
-ve ctrl
Control
TNF
300
200
100
ii
Expression relative to 18S
**
****
Control
TNF
Gpr4
Gpr65
Gpr68
Gpr132
Asic1
Asic2
Asic3
Asic4
Trpv1
Il-6